FREE

SEMI-ANNUAL REPORT NO. 2

DEVELOPMENT OF HIGH-TEMPERATURE CHROMIUM ALLOYS

by

J.W. CLARK and C.S. WUKUSICK

prepared for

GPO PRICE $ _____

CFSTI PRICE(S) $ _____

Hard copy (HC) 3.00

Microfiche (MF) .50

ff 653 July 65

NATIONAL AERONAUTICS AND SPACE ADMINISTRATION

Contract NAS3-7260

MATERIALS DEVELOPMENT LABORATORY

GENERAL ELECTRIC

FLIGHT PROPULSION DIVISION

NASA [redacted]

SEMI-ANNUAL REPORT NO. 2

DEVELOPMENT OF HIGH-TEMPERATURE CHROMIUM ALLOYS

by

J. W. Clark and C. S. Wukusick

Prepared for

NATIONAL AERONAUTICS AND SPACE ADMINISTRATION

APRIL 22, 1966

CONTRACT NAS 3-7260

Technical Management
NASA Lewis Research Center
Cleveland, Ohio
John P. Merutka, Project Manager
William D. Klopp, Research Advisor

GENERAL ELECTRIC COMPANY
Cincinnati, Ohio 45215

DEVELOPMENT OF HIGH-TEMPERATURE CHROMIUM ALLOYS

by J. W. Clark and C. S. Wukusick

General Electric Company

SUMMARY

Some 40 chromium alloys have been induction melted, cast as ingots of about four pounds each, and processed to small-diameter bar stock. In addition, over 150 compositions were arc melted as 50 to 100 gram buttons and were selectively evaluated with respect to critical properties. Several of the dilute, dispersion-strengthened alloys exhibited ductility at sub-zero temperatures combined with tensile strengths over 35,000 psi at 1900°F. Addition of 4 atomic percent Mo raises the tensile strength of carbide-containing alloys to about 60,000 psi at 1900°F, with the expected expense to low-temperature ductility. Additions of W are even more effective strengtheners, with tensile strengths of 81,000 and 30,000 psi at 1900° and 2400°F respectively being measured in a Cr-6W-.1Y alloy, but have a more detrimental effect on the workability than does Mo.

The most promising approach identified in the button alloys is the use of La to inhibit nitridation and consequent embrittlement during air exposure at elevated temperatures. Even compositions containing carbides rich in Cb or Ta, which otherwise are highly susceptible to nitrogen attack, resist such attack in alloys with additions of 0.3 to 0.5 atomic percent La. Lower concentrations are equally effective in alloys with Group IV A carbides, which have better inherent resistance to nitridation.

INTRODUCTION

The use of chromium as a base for elevated-temperature structural alloys has been limited in the past by its rather low strength, difficulties in melting and casting, the lack of ductility at low temperatures, and its further embrittlement during extended exposure to air at potential service temperatures (due primarily to a high reactivity with nitrogen). Earlier studies of induction-melted, wrought chromium alloys by this laboratory [1-3] have identified alloy systems which not only exhibited significant strength advantages over currently available superalloys at temperatures above about 1800°F, but which also gave indications of overcoming or reducing the severity of the aforementioned problems.

Using this prior work as a basis, it is the overall objective of the present research program to further extend the useful time-temperature-stress regime under which chromium alloys can be applied in advanced air-breathing propulsion systems. Several alloying approaches are being evaluated in terms of their effects on strength, ductility and nitridation resistance. These approaches have been described in some detail in the first semi-annual report [4] and need not be repeated fully here. Very briefly, five broad classes of alloys are included in the study. These five types of alloy systems, with examples of the additions being made, are:

1. Nitridation inhibitors (Y, Th, Hf)
2. Solid-solution strengtheners (Mo, W)
3. Solid-solution ductilizers (Re, Ru, Co)
4. Dispersion strengtheners (carbides, borides, intermetallics)
5. Complex combinations of above.

The experimental program is divided into Tasks I and II. Task I, with which this report is concerned, consists of the preparation and evaluation of some 60 to 65 alloys as heats of approximately four pounds each and some 150 alloys as small arc-melted buttons. Upon completion of Task I, the five compositions with the most useful combination of properties will be selected for consolidation as larger heats, and these alloys will be evaluated in greater detail in Task II.

TECHNICAL APPROACH

In several instances, sufficient data are available from prior work to specify compositions which merit full evaluation in Task I. In other cases, this prior work has identified potentially fruitful alloying approaches, but has not proceeded to the point that exact compositions can be recommended with confidence. In the latter instances, it was considered more efficient to first conduct surveys of such alloy systems using heats of smaller size and confining the evaluation to the most critical characteristic(s) affected by the variable under study. This approach was adopted for this program, and four separate phases of alloy design are being undertaken in Task I:

A. First series of induction-melted heats (3-4 pounds).
B. Small heats for system surveys (50-100 grams).
C. Series of induction-melted heats based on A. and B.
D. Optimized compositions based on A through C.

Two somewhat arbitrary "standards" are employed in the initial phases of Task I. Briefly, the intent is to evaluate several alloying approaches using additions to or departures from the standard alloys. This standard could have been selected as unalloyed Cr or perhaps Cr-Y. Results from either of these would probably yield the same relative rating of the effectiveness of the further additions. The results would not, however, be likely to approach those required for the time/temperature/stress regime of interest here.

The standard solution-strengthened alloy, in atomic percent, is:
Cr-4Mo-.1Y (Cr-7.1Mo-.17Y in weight percent)

As might be expected, W has a considerably higher strengthening effect than Mo at elevated temperatures on an atomic basis. When the increase in strength per weight percent solute is considered, W and Mo are essentially equivalent at 2000°F and W is superior at higher temperatures. However, prior experience in these laboratories indicates that W additions are limited to about 4 atom percent by the solid-state miscibility gap in the Cr-W system [2]. More highly alloyed compositions reject a W-rich solid solution upon aging at temperatures below 1800°F and attempts to work such alloys have not been successful. Alloys with somewhat higher atomic concentrations of Mo have been reduced from ingot to bar stock and their strengths and oxidation properties are rather attractive. Therefore Mo alloys have been emphasized in preference to W in the initial phases of Task I. The Cr-4Mo-.1Y alloy selected as the standard alloy will provide an increase of some 20,000 psi in the 2000°F tensile strength over that of Cr or Cr-Y, yet should permit processing without undue difficulty.

The standard reactive-metal/carbon alloy, in atomic percent, is:
Cr-.05Y-.4Zr-.2Ti-.4C
(Cr-.085Y-.7Zr-.2Ti-.09C in weight percent)

The use of a Zr-rich combination of Zr and Ti as the carbide-stabilizing addition represents the approach which has yielded the best balance of critical properties in our prior work [1,2]. This type of carbide is used as the standard in Phases A and B of Task I. Volume fractions of the dispersed phase, reactive-metal to interstitial ratios, and compositions of the compound-stabilizing elements have been varied with this standard as the basis for comparison. A limited evaluation of borides is also being performed.

Finally, the desired level of retained yttrium is dependent on the type of alloy under consideration. Binary alloys with residual Y levels of 0.3% and higher are quite easy to work and have good oxidation resistance. Additions of substitutionally soluble elements do not markedly reduce the tolerance for Y, particularly in the case of non-reactive solutes. Carbide-strengthened alloys on the other hand, are hot-short and suffer intermediate-temperature nitridation and consequent embrittlement at Y contents above 0.2% and most considerations indicate that the optimum level may be more nearly 0.1%. Microprobe scans of such alloys and emission analyses of extracted phases show a lower solubility of Y and/or a tendency to segregate to the carbides. For these reasons, an intended Y level of .17% (.1 atom %) is used as a standard in the Phase A alloys which do not contain soluble second phases such as carbides, and a lower level of .085% Y (.05 atom %) has been established as the standard in the dispersion-strengthened alloys.

A total of some 40 compositions which represent five general types of alloys have been selected for screening in Phase A. Consolidation of these alloys has been performed primarily by induction melting of H_2-reduced chromium

and casting as 2.125" diameter ingots. The ingots are processed by extrusion of Mo-canned billets followed by swaging to 0.25" diameter. Wrought bar stock from one representative alloy from each of the five types is subjected to:

1. A complete chemical analysis from three locations in the original ingot to document homogeneity.

2. A microstructural study of heat treatment response in the range 1400°F to values in excess of the solvus temperature of dispersed phases.

3. Low-temperature tensile tests in the three most attractive thermal conditions to determine the ductile-brittle transition temperature.

Heat treatment of the remaining alloys in Phase A is based on the above results. All the following are determined on all Phase A alloys:

1. Analysis for interstitials and yttrium to insure the combined O_2 plus N_2 content does not exceed 300 ppm total and that the retained Y level is in the intended range.

2. The ductile-brittle transition temperature in tension.

3. Elevated-temperature tensile strength in vacuum (in the range 1900°-2400°F) in one wrought and one fully recrystallized condition.

4. Air oxidation behavior in the range 1500° - 2400°F.

5. Metallographic evaluation of the above specimens.

In Phase B, several different alloying approaches are being studied in terms of specific effects on phase relationships, workability and low-temperature ductility, and resistance to nitrogen embrittlement. Consolidation of these compositions is by arc melting of small buttons or drop castings, and critical alloy interactions in each series are being investigated by selective microstructural analyses, oxidation, forging and rolling trials, and bend testing.

Results from Phase A and B will be used as the basis for design of more nearly optimized alloys in later phases of Task I. Approximately 20 compositions will be prepared and evaluated as in Phase A. In addition to the tests described above, 100-hour creep-rupture strengths will be determined at 2100° and 2400°F for those alloys which exhibit the best combination of other critical properties.

EXPERIMENTAL RESULTS - PHASE A

Consolidation

Analyses of raw materials used in melting the Phase A alloys are shown in Table I. All of the induction-melted heats were made from the hydrogen-reduced electrolytic flake. The iodide chromium was used only in preparation of high-purity unalloyed chromium by extrusion and swaging of steel-sheathed crystals and a Cr-35Re alloy by arc melting.

Seven-pound alloy charges were used throughout the induction melting work described below. Total yttrium concentrations of 0.5 to 0.8% were employed, depending on the desired residual level. In each case the chromium, non-reactive solutes such as molybdenum or tungsten, and 0.4% yttrium were blended and cold pressed into cylindrical briquettes. The remainder of the yttrium and all reactive solutes, such as Group IV A and V A metals and carbon, were placed in a charging tray in the furnace for addition to the melt later in the cycle.

All alloys were melted in a 25 KW NRC vacuum induction furnace, which can accomodate heat sizes up to about 15 pounds. A Y_2O_3-stabilized ZrO_2 crucible was packed inside the induction coil with coarse ZrO_2 grit serving to insulate the crucible from the coil assembly. The crucible, which was used for only one melt and then replaced, was sealed to the assembly and a ZrO_2 pouring spout was machined and attached to the lip by a close mechanical fit. After loading the briquetted charge into the crucible, the furnace was evacuated to a pressure of about 10^{-2} torr. Leak rates, measured just before applying power to the coil, were approximately 10^{-5} torr per minute. Initial heating was performed under vacuum, until the charge temperature reached about 2000°F. Purified argon was then admitted to the chamber to a partial pressure of 650-700mm, and the remainder of the melting cycle was conducted in this inert atmosphere in order to reduce vaporization of the chromium. The power was increased to 15-18 KW until the charge was completely molten, which required 8-10 minutes from the time the argon was introduced. Power input was then reduced to 10-12 KW, resulting in a stable superheat of 100°-150°F. After holding the charge molten for 15 minutes under the static atmosphere of argon, the remainder of the yttrium and any other reactive solutes in the particular alloy were added from the charging tray. Each melt was stirred by rapid cycling between power settings of 12 and 20 KW, held for an additional 4-5 minutes, and cast with power on.

Charges were cast into copper molds fit with 2.125" diameter CaO-stabilized ZrO_2 mold liners and ZrO_2 hot-tops. The ceramic liners are necessary to prevent solidification cracks which occur in all but the most dilute alloys upon casting directly into copper chill molds. Hot-tops, which consumed about three pounds of the total charge, are necessary to prevent extension of the solidification pipe into the ingot. Thus sound ingots of about four pounds were obtained by this casting technique.

Nominal compositions of the induction-melted alloys of Phase A are presented in Table 2, which also includes analyzed gas, yttrium, and zirconium contents. In alloys which contain no intentional zirconium addition, the latter analysis is indicative of the degree of reaction of the melt with the stabilized ZrO_2 crucibles and mold liners. In general, pickup of only a few hundred ppm Zr occurred. Gaseous impurities are well below the limit of 300 ppm established for this program. Revisions in the melting and casting practice have effectively eliminated the drastic contamination experienced in the first series of heats of these alloys [4]. Yttrium retention is generally within the intended range, but in a few instances very low residual yttrium levels were recorded. This behavior, which parallels earlier experience [2, 3], reflects the high reactivity of yttrium with impurities such as oxygen and is associated with minor differences in slag formation from heat to heat.

Cast microstructures of several alloys are shown in Figure 1. (The composition of the "Kromic" acid etchant is shown in Appendix A). The CI-1 alloy is representative of the Cr-Y and Cr-M-Y series where M is a non-reactive substitutional solute such as Mo or W. In such alloys isolated intergranular particles, presumably Y-rich, are observed and there is some intragranular pitting as shown in Figure 1A. The Cr-4Re-.1Y alloy in Figure 1B exhibits in addition a semi-continuous grain-boundary phase in some areas. Since this Re concentration is far below the solubility limit and the residual Y content is quite low, it is possible that this phase is a complex oxide rich in Re. The suggestion of eutectic freezing at the triple point shown would tend to support this possibility.

Alloys with the standard ZTC (Zr-Ti-C) addition have the appearance illustrated in Figure 1C. An intergranular carbide network, which previous work [2, 3] has shown to be rich in ZrC, is formed upon solidification. A much finer carbide dispersion, rich in TiC, precipitates throughout the matrix during cooling. Alloys which contain as the carbide-stabilizing addition only Zr and/or Hf, each of which has rather restricted solubility in chromium [4, 5], exhibit the same type of intergranular network but form only a few finely dispersed carbides in the as-cast condition, as shown in Figure 1D.

Carbide-containing alloys that have more highly soluble [6, 7] stabilizing additions such as Ti, Cb, or Ta have much less pronounced intergranular networks and also form a more general intragranular distribution of fine carbides as shown in Figures 1E and 1F. It will be shown in following sections that the strengths of such alloys are considerably higher than those which contain only ZrC or HfC additions.

Processing

After grit blasting to remove remnants of the ZrO_2 mold liner, each of the ingots was cropped by power hacksaw at the junction with the hot-top. Prior

to extrusion, the ingots were encased in protective cans with an OD of 2.06". The dilute alloys, those which contained no major substitutional solutes, were canned in mild steel and the remainder in molybdenum. They were machined from as-cast diameters of 2.2 $\pm$ .1" to billet diameters of 1.9 $\pm$ .05", the exact dimensions being governed by the ID of the can. Lids were welded to the cans by the tungsten arc process in a vacuum-purged chamber back-filled with high purity helium, then the cans were evacuated and sealed by electron beam welding.

All of the first group of alloys were extruded from 2.13" diameter containers through 0.75" diameter dies. A summary of the extrusion data is presented in Table 3. Heating was performed in an induction unit under a protective atmosphere of argon. The canned billets were soaked for 10 minutes at temperature, then transferred to the container of a 1250 ton hydraulic press (Lowey Hydropress) with handling times of 10 to 15 seconds. Lubricants were powdered glass plus a mixture of necroline and graphite. The tool steel dies were flame sprayed with ZrO_2 to reduce wash and extend their useful lives. Solid graphite back-up blocks were inserted behind the billets to reduce the extent of the extrusion defects in the trailing ends. Inspection of the extruded stock was performed by radiographic and fluorescent penetrant techniques. Other than minor nose bursts and the typical trailing-end defects, no internal flaws were detected.

Processing to final dimensions was accomplished by swaging. The general procedure in swaging to 0.25" diameter involved careful inspection of individual 3" lengths of extrusion by macroetching, fluorescent-dye penetrant, and in some cases, metallographic techniques to ensure sound starting material. Initial swaging of the billets, with the protective jacket intact, was performed at temperatures ranging from 150° to 250°F below the extrusion temperature, the smaller temperature reductions being used for the more complex alloys. Heating was done in molybdenum-wound tube furnaces under a protective atmosphere of flowing hydrogen. Heating between passes was limited to 3 to 5 minutes and any cracks which were observed during working were cropped while the material was still hot, using a high-speed cut-off wheel. The bar stock was reduced to approximately .47" diameter under these conditions, then straightened in long-stroke dies, and given a short stress relief at the swaging temperature.

Finish swaging to 0.25" was conducted at 1900°F for Cr-Y and related alloys, at 2050 $\pm$ 50°F for the dilute carbide- or boride-containing alloys, and wherever possible at 2200 $\pm$ 50°F for the more complex compositions. Some sections of the latter, because of extensive cracking at 2250°F, had to be finish swaged at somewhat higher temperatures but all alloys were worked to final dimensions below 2400°F.

Microstructures of typical compositions in the final wrought condition are shown in Figure 2. The Cr-.10Y alloy CI-1 shows a considerable amount of polygonization and some evidence of recrystallization after swaging at 1900°F. The high-purity Cr-35Re alloy in Figure 2B is completely warm worked, with no

sub-boundaries evident after final working at 2200°F.

As was the case in the cast condition, there is some non-uniformity in the distribution of the finer carbides in the as-worked Cr-.05Y-ZTC alloy pictured in Figure 2C. It should be pointed out in this respect that one-hour annealing at 2000° to 2200°F causes additional precipitation of fine carbides in the regions between the bands of particles in the swaged structure such that a much more uniform dispersion is obtained. The Cr-.05Y-HZC alloy CI-21, which in the cast condition shows only a coarse intergranular carbide network, exhibits a uniform but rather widely spaced dispersion of finer carbides after working at 2000°F as indicated in Figure 2D. Further aging at 2100° ± 100°F is also effective in this alloy in promoting a still finer dispersion but, at least in optical microscopy, the interparticle spacing appears to be too great for most effective dispersion strengthening.

The finest carbide dispersions in the wrought alloys are observed in systems in which the carbide-stabilizing element has a greater solubility in Cr than either Zr or Hf. Examples of such compositions, which include Ti-, Cb-, and Ta-rich reactive metal additions, are shown in Figures 2E and 2F.

A summary of the effect of processing on the microhardness of the Phase A alloys is shown in Table 4. Note that in the carbide-containing Cr-4Mo alloys, the greatest hardening from the cast to the swaged condition occurs in those alloys with the higher concentrations of those reactive metals which promote formation of fine carbides. All of the alloys with major substitutional solute concentrations at or below 4 atomic percent were worked to 0.25" diameter without undue problems. As reported previously [4], however, some of the more highly alloyed compostions could not be worked by conventional techniques. In general, alloys with cast or extruded hardnesses above about 330 DPH fell into this category. Such alloys that could not be swaged directly were impact extruded from 0.75" to 0.375" diameter at 2450°F prior to further swaging attempts. The compositions that were so worked are designated in Table 4. Where a final swaging temperature is listed for the impact extruded alloys, two to four mechanical test specimens were successfully produced. Those that could not be swaged to final dimensions in spite of the intermediate processing step have no entry under swaging temperature in the tabulation. Swaged hardnesses have not yet been measured on most of these impact extruded and swaged alloys. Un-strained portions of tested specimens will be used for this purpose in order to conserve the already highly limited material.

Response To Heat Treatment

Swaged sections of at least one representative alloy from each of the five general types under study were vacuum annealed for one hour at temperatures in the range 1400° to 3000°F using increments of 200°F. The results of these treatments in terms of the microhardness and recrystallization behavior are presented in Figure 3. The recrystallization temperature of the

Cr-Y alloy, approximately 1900°F for 50% recrystallization in one hour (based on metallographic observations), is increased by about 50°F by the addition of 4 atomic % Mo and by an additional 50° to 100°F by the (Zr, Ti)C dispersion. The concentrated Cr-Re solid solution has a considerably higher hardness and the recrystallization temperature, as defined here, is about 2300°F.

Each of the carbide-containing alloys exhibits a hardening peak at 2000° ± 200°F. As shown in Figure 3, this peak occurs in one-hour aging at about 1800°F in the Cr-Y-ZTC alloy and is increased to 2000°F by the addition of 4Mo. The effects of exposure in this temperature range on the microstructure are pictured in Figure 4. The Cr-Y-4Mo alloy with the (Hf, Zr)C addition was selected for illustrative purposes, since its as-swaged structure is virtually free of fine particles and the precipitation of carbides upon aging is more evident. Stability of the fine carbide dispersion in this particular alloy is rather low, with almost complete dissolution occuring in one hour at 2400°F. Complex carbides containing Ti, Cb or Ta resist dissolution or agglomeration to considerably higher temperatures.

In addition to the hardness and microstructural response, an exploratory investigation of the effects of selected heat treatments on the low-temperature tensile behavior of representative alloys was also conducted. Tests were made at a nominal strain rate of .03 per minute using a .120" diameter specimen with a 0.5" gage length provided with generous fillet radii. Prior to testing, specimens were electropolished in a 10% perchloric - 90% acetic acid bath maintained at or below 50°F. In general, an annealing temperature below the one-hour recrystallization temperature (1800°F), one at or near the aging peak for carbide-containing alloys (2000°F), and one above the recrystallization temperature (2400°F) were included in this portion of the study. The results are summarized in Table 5. It should be noted that the ductility of each of the dilute alloys with carbide additions is superior of that of the Cr-Y binary. The compositions with (Zr, Ti)C or (Hf, Zr)C dispersions are rather ductile at room temperature and exhibit measurable plastic flow at -50°F in both the wrought and fully recrystallized conditions. Their strengths are also considerably higher than that of CI-1. These simultaneous improvements in strength and ductility are a result of interaction of the carbide particles during working and/or annealing at 2000° ± 200°F with both residual interstitial impurities (the monocarbides exhibit complete solubility with cubic monoxides and nitrides) and with the dislocation array. During the coming report period, transmission electron microscopy and diffraction will be employed to better define these interactions in selected alloys.

Addition of 4 atomic percent Mo raises the ductile-brittle transition temperature (DBTT) by at least 200°F. The Cr-Y-4Mo ternary appears to be slightly more ductile than corresponding alloys with carbides but the difference, if real, is not great. Strengths of the compositions with carbide dispersions are at least 10 to 15% higher than their carbon-free counterpart at these temperatures, and show an even higher advantage at elevated temperatures as will be shown in the following section.

The best balance of strength and ductility was generally observed after a one-hour anneal at 2000°F. This temperature was selected for treatment of the rest of the Phase A alloys for initial screening of mechanical properties.

Tensile Properties

Most of the further screening tests conducted to date have been made on specimens annealed for one hour at 2000°F. Low-temperature testing procedures were described previously. Elevated-temperature tests were made on ground button-head specimens with an overall gage length of 1.1" and a diameter of .160". In each temperature range, an Instron machine was employed at a nominal strain rate of .03 per minute. Tests at 1900°F and above were made in vacuum at pressures of 10^{-5} torr or below.

Ultimate tensile strengths and reduction of area values from representative alloys are plotted as a function of temperature in Figures 5 an 6 respectively. The Cr-Y binary has quite low strength over the entire temperature range of interest. Addition of the (Zr, Ti)C dispersion results in an increase of at least 60% in these strengths at the higher temperatures, but the absolute values are still rather low. A concentration of 4 atomic percent Mo doubles the low-temperature strength of Cr-Y and raises its strength by a factor of 3 to 4 at 1900° to 2400°F. The increment due to the ZTC dispersion appears to be about the same in either a Cr-Y or a Cr-Mo-Y base. The CA-2 alloy (Cr-35Re) has considerably higher strength at 1900°F but at 2400°F, where the alloy is completely recrystallized prior to test, the strengthening by the concentrated Re addition is not much greater than that afforded by 4 atomic percent Mo.

Based on the criterion of 5% reduction of area defining the transition from brittle to ductile behavior, the DBTT of Cr-Y and Cr-Y-ZTC alloy is near or below room temperature and that of the Cr-4Mo-Y composition about 300°F. Low-temperature tests have not yet been conducted on the other two alloys shown in Figure 6, but the Cr-35Re alloy is of course expected to be ductile below room temperature.

All of the available tensile results after one-hour annealing at 2000°F are presented in Table 6. Strength and ductility data from the strongest alloys of each type are compared to the C-207 alloy developed by this laboratory [2,3] in Figures 7 and 8. The 1900° and 2400°F strengths of 81,000 and 30,100 psi measured in the Cr-6W-.1Y alloy CI-8 represent the highest strengths reported to date for a chromium base alloy. These values are nearly double the strength of C-207, which itself provided a significant advantage over other chromium alloys at the time of its development.

It will be noted, where direct comparisons are available in Table 6, that W is a considerably more effective strengthener than Mo on the basis of atomic concentration. However, as mentioned in an earlier section, alloys with 8

atomic percent Mo or with 6 to 8 atomic percent W and W plus Mo are among those which could not be swaged directly from the extruded condition, and even the alloy with 4 atomic percent W was rather difficult to work. The few tensile tests reported in Table 6 represent the only useful bar stock which was obtained from such alloys, and most of it was worked only by impact extrusion prior to final swaging. It is clear that solute concentrations above 4% W or 6% Mo are quite effective with respect to strength, but their adverse effect on workability may limit their practical application. Since W is more favorable in its strength characteristics and Mo in its workability behavior, consideration will be given to simultaneous additions of these two solutes to carbide-containing alloys at the combined level of 4 to 6 atomic percent in the extension of the work into later phases of Task I.

The carbide-containing Cr-4Mo-Y alloys all exhibit elevated-temperature strength increases over the base composition. This advantage is least in the ZTC alloy at the higher Y concentration (CI-30), which parallels earlier observations that Y has a weakening effect in alloys with dispersed carbides at higher temperatures [1-5]. Although subsequent alloys containing carbides rich in Ta, Cb, and Ti are exptected to be even stronger because of their finer carbide dispersions, the highest strengths observed to date in the Cr-4Mo base are those in the low-Y ZTC alloy CI-29 and in the HZC alloy CI-37. As shown in Figures 7 and 8, the strength of the latter composition is higher than that of C-207 by 30% or more, the DBTT is about the same (350° to 400°F) and the ductility at higher temperatures is considerably greater.

It is worthy of note in Figure 8 that the ductility of the dilute Cr-Y-HZC alloy CI-21 is quite good at low temperatures. Alloys with boride dispersions also have rather attractive properties. Substitution of boron for the carbon in otherwise identical compositions (CI-22 and CI-23) results in some increase in strength accompanied by what appears to be a relatively minor loss of ductility, as shown in Table 6. More complex boride alloys will be included in later phases of the study.

Tensile tests of the remainder of the Phase A alloys are currently being conducted. In addition to completing evaluation after the 2000°F treatment, specimens from each alloy (except those with limited supplies of bar stock) are being tested in the fully recrystallized condition after annealing for one hour at 2400°F.

Air Oxidation Behavior

Oxidation tests in air at 1500°, 2100° and 2400°F have been or are being made on all of the Phase A alloys. Analysis of these data, which includes microscopic examination and measurement of the extent of sub-surface hardening, is not sufficiently complete at this writing to justify tabulation. Several important trends, however, have become apparent. Carbide-containing Cr-Y or Cr-Mo-Y alloys which have only Zr and/or Hf as the carbide stabilizing addition do not form sub-surface nitride layers and are not internally hardened in 100

hours at either 1500° or 2100°F and are much more resistant to nitridation at 2400°F than similar alloys containing Cb, Ta or Ti. It also appears that the binary Cr-35Re alloy is resistant to nitridation at each temperature even in the absence of Y, although there is evidence of formation of a volatile oxide on this composition. The dilute Cr-Y-Th-Hf alloy CI-3 is highly resistant to both oxidation and nitridation at 1500° to 2400°F, as demonstrated in an earlier study [8]. These and related factors have been explored in some detail in several systems of Phase B and will be included in the design of alloys for following portions of the study.

EXPERIMENTAL RESULTS - PHASE B

Data from a rather large number of arc-melted buttons from several alloy systems have been generated in this portion of the program. The ultimate goal is to select the most promising of the approaches surveyed here for incorporation in larger heats to be prepared in subsequent phases of the study. Some of the results that have been presented previously [4] will be summarized again here for convenience to the reader. All the alloys in Phase B were arc melted as 50 to 100 gram heats using tungsten electrodes, water cooled copper button or drop-casting molds, and a helium-argon atmosphere gettered prior to preparation of the buttons by melting a titanium charge. Except where noted, the alloys were melted a minimum of three times to promote homogeneity.

Cr-W-V Alloys

Tungsten is one of the most effective solid-solution strengthening additions for chromium but, as a result of the miscibility gap in the Cr-W system [6], the solubility of W in Cr is only about 5 atomic percent. Prior work indicates that vanadium exerts only a mild strengthening effect, but that it increases the solubility of W in ternary alloys [9]. Since available data were too limited to establish the solvus with any degree of accuracy, a series of alloys with 5, 7.5 and 10 atomic percent W was prepared with V additions ranging from 0 to 20%. The alloys were arc melted from iodide Cr crystals and drop-cast as 0.5" diameter cylinders. All alloys were single phase as-cast and after 2-hour annealing at both 2500° and 2900°F. The higher temperature was necessary for complete homogenization because traces of coring were present after 2 hours at 2500°F. Homogenized specimens were subsequently aged 230 hours at 1650°F and 24 hours and 200 hours at 1800°F. The longer time at 1800°F was necessary to cause uniform precipitation in the two-phase alloys.

Cr-W-V alloy compositions and metallographic observations are given in Table 7. In the binary alloys, a sharp increase in hardness between 7.5 and 10% W was accompanied by irregular precipitation of what is presumably a W-rich solid solution. In the ternary alloys the precipitation was general

and relatively uniform as indicated in Figure 9. It is difficult to determine whether the amount of precipitate is increased with increased V concentration. The precipitate particles are apparently very small and the difference in apparent precipitate density may be caused in part by the relative rates of etching of grains of differing orientations. In general, however, there appears to be an increase in degree of precipitation as the V concentration is increased.

In the more dilute ternary alloys a slight softening occurred upon first appearance of the precipitate, while in the more concentrated alloys hardening was observed. Location of the alloys in relation to the proposed ternary Cr-W-V equilibrium diagram[9] is shown in Figure 10. The present results strongly indicate that V does not increase the solubility of W in Cr at low temperatures. It is not clear, however, whether a miscibility gap also exists in the Cr-V binary system or whether V simply increases the rate of precipitation of W from the Cr solid solution. The hardness data support the former suggestion, i.e., a miscibility gap exists in the Cr-V binary system. Precipitation of a V-rich phase would not be expected to result in the large hardness increase that has been noted in the Cr-W binary alloys when the W-rich solution precipitates.

The uniformity and the apparent small size of the precipitate in the V-rich alloys may provide a significant effect on the strength and/or ductility. A large heat of a ternary Cr-W-V alloy has been planned for Phase C of this study to more fully evaluate the effects of heat treatment on the mechanical properties.

Co Additions To Cr-Re And Cr-Ru Alloys

Concentrations of about 35 atomic percent Re[10] and 20 atomic percent Ru[11] result in highly ductile Cr alloys. As previously pointed out[4,12], additions of 25 to 30 a/o Co result in similar improvements in ductility when the alloys are supersaturated by chill-casting or by quenching from an annealing temperature above 2500°F. The solubility of Co in Cr drops rapidly with decreasing temperature, however, so that the alloys are embrittled by sigma-phase formation during aging in the temperature range of 1500° to 2000°F.

The approach adopted in the present series was to add Co to Cr-Re and Cr-Ru alloys in an attempt to decrease the amounts of Re or Ru required for significant ductility improvements. As previously reported[4], Co can be substituted for relatively large portions of the Re and Ru required to promote cold workability in cast Cr alloys. Thermal stability is impaired by such substitution, however, particularly at the high Co levels.

In order to further define the Cr solid solution region in the Cr-Re-Co ternary system, an additional series of alloys located near the tentative 1650°F phase boundary was prepared. Alloy compositions and metallographic data are presented in Table 8. One of the alloys (30 Re-5.7 Co) contained a precipitate after 2-hour homogenization at 2750°F, but the remaining alloys

were single phase. After aging for 100 hours at 1650°F all but two of the alloys exhibited a grain boundary precipitate, presumably sigma phase. The microstructure of one such alloy is shown in Figure 11 along with the structures of alloys of higher Co contents which exhibit better ductility in the supersaturated condition but poorer stability at 1650°F. The extent of the Cr solid solution region in the Cr-Re-Co system at 1650°F is shown in Figure 12.

Alloys listed in Table 8 were forged at 2200°F but most, particularly those high in Co, fractured badly during forging. Attempts to cut bend test specimens from the forged alloys were not successful because of their brittleness except in the case of the Cr-2.5Co-25.6Re alloy. The latter composition exhibited ductility at room temperature (approximately 20° bend of a .050" thick specimen at a bend radius of .060" before fracture). The results indicate that the substitution of Co for Re in Cr alloys is not practical because of the instability of the alloys at intermediate temperatures (~ 1650°F). Co-rich alloys located near the solvus line, while stable, are very brittle. No further work will be performed on the ternary Cr-Co-Re or Cr-Co-Ru alloys.

Cr-Y Alloys With Dilute Re, Ru And Co Additions

Aside from the improvement of ductility in concentrated solutions, Re has been shown in prior work to have a beneficial effect on air oxidation behavior of much more dilute Cr alloys containing Y [1, 8]. Since Ru and Co are analogous to Re in other respects, the oxidation-nitridation resistance of a series of Cr-Y alloys with relatively small additions of these three elements was evaluated. The alloys were prepared from hydrogen-reduced Cr flake and purified Re, Ru, and Co. The Cr was alloyed first with the Re, Ru, or Co to insure homogeneity. These buttons were crushed to provide a master alloy to which the Y was added. The alloys were first melted as buttons and drop cast into 0.5" diameter cylinders. Disks approximately 0.1" thick were cut, ground through 600 grit paper, cleaned, and exposed to air at 1500°F-100 hours, 2100°F - 100 hours, and 2400°F for 24 hours. In general, as reported in detail in an earlier report [4], the combination of Y and Re results in improved oxidation-nitridation behavior. The Cr-Re-Y alloys exhibited better oxide adherence and much less nitridation than similar compositions with either Ru or Co. Only Re-containing alloys are included in the extension of this work into Phases C and D.

Cr-Y Alloys With Group IV A And V A Carbides

In order to provide the best possible combination of strength, ductility, and resistance to embrittlement during air oxidation in the design of dispersion-strengthened alloys in succeeding phases of the work, a critical survey of the interactions between carbide-forming elements and nitridation-inhibiting additions is being made in Phase B. Results from the first portion of that survey are presented in this section. Each of the Group IV A and Group V A metals were added at levels of 0.5 and 1.0 atomic percent to

base compositions of Cr, Cr-Y, and Cr-Y-C. The alloys were arc melted as 60-gram buttons, sheathed in mild steel and drop-forged at 2200°F to a 60% reduction in thickness. The alloys with reactive metal additions of 1.0 atomic percent were rolled to .070 ± .010" strip at 2100° - 1900°F, using initial reductions of 20% per pass at the higher temperature and finishing with 10% reductions at 1900°F.

Test results from this series have been reported previously [4], but since they have a direct bearing on subsequent sections of this report, they are summarized here for the reader's convenience. Data from 2100°F oxidation tests of the entire series are shown in Table 9 and mechanical properties of representative alloys are summarized in Table 10. Rather marked differences in both oxidation and mechanical behavior are observed between those alloys containing additions of Group IV A metals (Ti, Zr and Hf) and those with solutes from Group V A (V, Cb and Ta). Each of the elements in binary alloys with Cr at the level of 0.5 atomic percent results in an increase in the oxidation rate over that of the unalloyed metal at 2100°F. However, small additions of Y to the alloys with Group IV A solutes are very effective in reducing oxidation, whereas Y is relatively ineffective when added to binary alloys with V, Cb, or Ta. The same trends are observed in similar alloys with C. Even without Y, the alloys with ZrC and HfC exhibit weight-gain values considerably below those with the other four carbides. Additions of Y, in general, result in lower oxidation rates in those compositions which contain carbides based on the Group IV A metals, but have little effect on alloys with Group V A carbides. The alloys with VC are an exception to this trend, in that quite low weight gain values are obtained in the presence of Y, particularly at the higher nominal concentration of 0.2 atomic percent. It should also be noted that the alloys with carbides based on Group IV A metals have somewhat lower rates of oxidation at the higher metal-to-carbon ratio, while the reverse appears to be the case for those with carbides of V, Cb, and Ta.

Differences in low-temperature mechanical properties and in the effects of oxidation on ductility, which are summarized in Table 10, are also pronounced. Alloys with TiC, CbC and TaC have considerably higher strengths and somewhat higher DBTT values in the rolled and annealed condition. Air exposure at 1500° and 2100°F results in a sharp decrease in ductility, particularly in the case of the CbC and TaC alloys. The compositions which contain ZrC, HfC and VC are ductile near or below room temperature and the former two types exhibit much better retention of ductility after air oxidation. DBTT values of 200° to 400°F were measured in oxidized Cr-Y-C alloys with Zr or Hf, compared to greater than 800°F in similar compositions containing Cb or Ta.

Some of the factors which are involved in the differences in both mechanical and oxidation behavior can be illustrated by the photomicrographs in Figure 13. Carbides in the alloys with Zr, which are typical in this respect of those with Hf, are rather coarse and widely spaced. This morphology results from the restricted solubility of Zr and Hf in Cr [5]. Carbides are

formed as grain boundary networks during solidification. These intergranular carbides are fragmented during processing, but are not appreciably altered by heat treatment. Such a coarse distribution does not have a large effect on either strength or ductility in the rolled and annealed condition. The particles are also too widely spaced to influence reaction during air exposure. Note in Figure 13A that only those few particles which intersect the surface appear to be affected by oxidation at 1500°F. At the higher oxidation temperature, the large carbides act as sinks for the gaseous contaminants as shown in Figure 13B, and no surface or intergranular nitrides are formed.

Carbides in the alloys with Cb or Ta additions are present in the form of fine, uniform dispersions which are much more effective in increasing the strength and result in somewhat lower ductility in the rolled and annealed condition. The further losses in ductility during intermediate-temperature air exposure are probably related to additional precipitation of interstitials, both from the matrix and from inward diffusion of oxygen or nitrogen, and a resultant interaction with the dislocation array. Although essentially no subsurface hardening was observed at 1500°F in the Cr-Y alloys with ZrC or HfC additions, those containing Cb or Ta were hardened by 25-50 DPH to depths of 4 to 6 mils. Oxidation at the higher temperature results in accelerated reaction of alloys with CbC or TaC dispersions. The particles are closely enough spaced that they present a semi-continuous oxidation front. They are rapidly saturated by the gaseous contaminants, and both surface and intergranular nitrides are formed as illustrated in Figure 13D. Even in the absence of C, additions of Cb and Ta appear to at least partially negate the beneficial effects of Y on oxidation behavior, as indicated by the weight gain data in Table 9. As noted previously, this is not the case with solutes from Group IV A.

Alloys with VC appear to have the poor features of each type discussed above, without the attractive properties of either. A relatively fine dispersion is formed during cooling from high temperatures, but the thermal stability is quite low. Rapid agglomeration occurs upon heat treatment at temperatures as low as 2000°F. Although the ductility of the alloys with V is good, their strengths are not greatly different than those of a Cr-Y binary and they are severely embrittled by oxidation at 2100°F. Structures of the alloys with TiC are similar to those with CbC in that a fine dispersion is formed. Embrittlement due to oxidation is not as great, however, since Ti additions, unlike those of Group V A solutes, do not interfere with the effects of Y.

Based on this survey, the choice of a combination of Zr and Ti as the "standard" carbide-stabilizing addition in the initial phases of Task I appears to be justified. Superior strengths, however, can be attained with Cb-rich or Ta-rich carbides. It is possible that embrittlement of such alloys can be minimized by the identification of an element which provides more effective resistance to oxidation and nitridation than does Y. Results of a study of this factor are presented in a following section.

Intermetallic Dispersion Systems

Two binary systems and one ternary were surveyed to establish the efficacy of intermetallic compounds as dispersion strengtheners and to measure the oxidation-nitridation resistance of the resultant alloys. The Cr-Cb, the Cr-Si, and theternary Cr-Cb-Si systems were selected for these purposes. In an effort to improve oxidation resistance, a Cr-0.1 Y base was used in most of the alloys. The elements were first added separately in arc melted buttons in sufficient amounts to produce $CbCr_2$ and Cr_3Si. Earlier work by Goldschmidt and Brand[13] had indicated that addition of the two elements in combination led to precipitation of $Cb_{0.6}Cr_{0.4}Si$ although the phase boundaries were not well established.

A summary of the observations made on these alloys is presented in Table 11 and typical microstructures are shown in Figure 14. Reasonably fine and uniform dispersions were achieved in alloys with Cb levels of 3 atomic percent and above and the precipitate appeared to be stable through 2200°F. However, when the Cb concentration is high enough to produce $CbCr_2$, the air oxidation behavior is particularly poor as shown in Figure 14B. The Cr-Si buttons, although exhibiting considerably better oxidation behavior, were quite brittle and fractured rather badly during forging in spite of their relatively low hardnesses. The workability of ternary Cr-Cb-Si alloys proved to be somewhat improved over those of the Cr-Si system, but oxidation and nitridation rates are still unacceptably high as shown in Table 11 and illustrated in Figure 14F. Unless alternate nitridation inhibitors with considerably greater effectiveness than that of Y can be identified, no further work on these systems is recommended.

Alternate Nitridation Inhibitors

As reported previously[4], La, Pr, and possibly mischmetal (50% Ce+ 50% La, Pr, Nd) were found to be more effective nitridation inhibitors than yttrium in a Cr-4 Mo matrix. During the present report period the work was extended to more complex carbide-containing alloys.

The first group of alloys containing various carbides and nitridation inhibitors are listed in Table 12 along with the oxidation test results. The alloys were drop cast from electrolytic Cr charges and then forged 50 to 75% at 2200°F. Oxidation test specimens were cut, polished and exposed in the

as-forged condition for 100 hours at 1500° and 2100°F and for 24 hours at 2400°F.

In general, the alloys containing carbides plus gettering additions exhibited hardening of 50 to 100 points DPH near the surface at 1500°F, although no evidence of nitride precipitation was noted at this temperature. Some intergranular oxidation occurred in the Cr-TiC-La alloy.

At the higher temperatures, La appeared to be the most effective of the additions evaluated in preventing nitridation. The effects of only 0.2 atomic percent La in preventing nitridation at 2100° and 2400°F in a Cr-ZTC alloy are shown in Figure 15. Thick nitride layers were formed on the base Cr-ZTC alloy while little or no nitridation occurred in the Cr-ZTC-0.2La alloy. A concentration of 0.2% La was also effective in preventing nitridation in the Cr-TiC alloy as shown in Figure 16, although the surface oxide was quite irregular. In the Cr-CbC alloy, additions of 0.2 La (or Pr) were not effective but additions of 0.5 La resulted in significant improvement as shown in Figure 16. Pr was similar to La in its effect on nitridation and the Cr-CbC-0.2La was nearly identical in appearance to Figure 16B.

In the binary Cr-La alloys, no evidence of incipient melting was detected at the level of 0.2 atomic percent La, but incipient melting did occur in the Cr-0.5% La alloy at 2100° and 2400°F. Available data on the Cr-La phase diagram indicate an eutectic temperature of about 1650° to 1700°F and the solubility of La at 2200°F is variously reported from 0.6 to less than 0.05 atomic percent. In order to better establish the solubility of La and the melting relationships, additional Cr-La alloys were produced from high-purity (iodide) chromium. Alloys containing 0.1 to 0.5 atomic percent in increments of 0.1 atomic % were drop cast, warm rolled at 1550°F, then annealed at 1650°, 2000°, and 2250°F. Metallographic examination indicated that the solubility of La in Cr is less than 0.1% in that a second phase was present in all alloys and agglomeration of this phase occurred in all the alloys at the higher temperatures. Incipient melting occurred at 2000° and 2250°F in the 0.4 and 0.5 atomic percent La alloys. At this writing it is not clear whether incipient melting occurred in the alloys which contained less than 0.3% La although agglomeration did occur.

In evaluating the effect of La on the structure, the purity of the starting materials must be considered. It appears likely that in the alloys made from the lower purity Cr, a large part of the La may be present as interstitial compounds and thus does not result in incipient melting but is still effective in innibiting nitridation.

Cr-Mo-La Alloys With Selected Carbides

An additional series of complex alloys containing 4% Mo, La and various carbides was prepared and partially evaluated for oxidation resistance. The

chemical compositions are given in Table 13 along with the results of air oxidation tests performed to date. An initial test at 2400°F was performed on as-cast specimens cut from the drop castings. The drop castings were then sheathed in Mo and swaged at 2400°F, but broke up badly. Sections of the swaged alloys were surface conditioned and oxidized at 2100°F for 100 hours. The specimens were irregular in shape so that weight-change data could not be obtained, but subsurface reactions were followed metallographically. Microstructures of several of the alloys after testing at 2100°F are shown in Figure 17.

In general, the alloys which contained carbides of Zr or Hf exhibited good resistance to nitridation in both the as-cast and hot-worked conditions. The alloys which contained Cb or Ta carbides exhibited very poor oxidation-nitridation resistance in the as-cast condition. In the alloys containing CbC the resistance apparently decreased as the La concentration was increased from 0.3 to 0.4 atomic percent. In the wrought condition, however, the reverse is true, apparently because working tends to break up the continuous Cb-rich carbide films in the grain boundary. The nitridation resistance of the wrought Cr-4Mo-CbC-0.4La alloy appeared similar to that of the Cr-CbC-0.5La alloy (compare Figures 16D and 17D) except for some internal oxidation in the Cr-Mo composition.

The results obtained to date indicate that in complex alloys containing Cb or Ta carbides, an addition of from 0.3 to 0.5 atomic percent La is required to provide nitridation resistance. In alloys containing carbides rich in Zr or Hf, 0.2 to 0.3% La is effective. The verification of the superiority of La as a nitridation inhibitor is considered to be potentially very important to the design of improved chromium alloys. This factor will be emphasized in Phases C and D of the present program.

CONCLUSIONS

1. Complex chromium alloys were successfully induction melted, cast, extruded, and swaged to 0.25" barstock. Interstitial impurity contents were maintained below 200 ppm total by revised consolidation techniques. Alloys with additions of 4 atomic percent Mo or W were processed without difficulty, but major solute concentrations of 6 and 8 atomic percent made necessary an intermediate working operation (impact extrusion) in order to produce even a limited supply of bar stock.

2. Several dilute carbide-containing and boride-containing alloys exhibited considerable ductility at room temperature and measurable plastic flow at 0°F and below in both the wrought and fully recrystallized conditions. Depending on the nature of the dispersion, some such alloys combined this low-temperature ductility with tensile strengths as high as 35,000 to 40,000 psi at 1900°F. Addition of 4 atomic percent Mo to the dispersed-carbide alloys increased the tensile strength at 1900°F to about 60,000 psi but raised

the DBTT to 300° to 400°F. The highest strengths to date were observed in a Cr-6W-.10Y alloy, which had tensile strengths of 81,000 and 30,100 psi at 1900° and 2400°F respectively. W is definitely superior to Mo with respect to strengthening, but appears to have a more adverse effect on workability.

3. Resistance to oxidation and nitridation was shown to be attractive in Cr-Y or Cr-Mo-Y alloys with Zr-rich or Hf-rich carbides. The binary Cr-35Re alloy appeared to have excellent air oxidation resistance in preliminary tests, and dilute Cr-Re-Y alloys showed promising air oxidation behavior at Re levels as low as 4 to 8 atomic percent.

4. Contrary to previously published information, V does not increase the solubility of W in Cr. In fact, some evidence was observed of a miscibility gap in the Cr-V binary system.

5. Substitution of Co for much of the Re in ductile Cr-35Re alloys resulted in cold workability in single phase alloys in the cast condition. These Cr-Re-Co compositions, however, were subject to profuse sigma precipitation and consequent embrittlement upon aging at 1600° to 1800°F due to a rapid decrease in the Co solvus with decreasing temperature. Such alloys, therefore, do not appear to be practical.

6. Dilute Cr-Y alloys with CbC, TaC, and TiC additions had finely dispersed carbides and exhibited attractive strength characteristics. The oxidation-nitridation resistance of such alloys, however, was markedly inferior to those with ZrC or HfC dispersions. Their reliable use will require a more effective means of preventing nitrogen embrittlement than that afforded by Y.

7. No attractive compositions were identified in the Cr-Cb-Si system or its binary components. Cr-Si-Y alloys were rather brittle and the poor air oxidation resistance of Cr-Cb-Y alloys was still evident after addition of Si.

8. Additions of La were shown to be quite effective in preventing nitridation in complex alloys containing carbides as well as in simple Cr-La and Cr-Mo-La compositions. Somewhat higher concentrations of La were required in order to promote nitridation resistance in alloys with CbC or TaC dispersions than in alloys with Zr-rich carbides. Because of a low solubility in Cr and some evidence of a rather low eutectic temperature, potential problems in consolidating La alloys were established, but its beneficial effect on air oxidation behavior is pronounced.

ACKNOWLEDGEMENTS

The authors wish to express their thanks to many colleagues who contributed to various phases of the work. Particular appreciation is extended to F. E. Walker, J. R. Kittle and R. J. Burgdorf.

REFERENCES

1. C. T. Sims & J. W. Clark, "Carbide-Strengthened Chromium Alloys" Trans. Met. Soc. AIME 230 (1964) 1168.

2. J. W. Clark "Preparation and Properties of a Carbide-Strengthened Cr-W-Y Alloy", General Electric Report R64FPD119, April 1964.

3. J. W. Clark & W. H. Chang, "New Chromium Alloys", paper presented at AIME High-Temperature Materials Symposium, February 1966 (To be published).

4. J. W. Clark & C. S. Wukusick, "Development of High-Temperature Chromium Alloys", Semi-Annual Report No. 1, NASA CR-54486, October 1965.

5. R. F. Domagala, "A Study of the Solubility of Zr in Cr" Trans. ASM 56, (1963) 878.

6. M. Hansen & K. Anderko, Constitution of Binary Alloys, 2nd Edition McGraw-Hill, New York, 1958.

7. R. P. Elliott, Constitution of Binary Alloys, First Supplement, McGraw-Hill, New York, 1965.

8. C. S. Wukusick, "Research on Chromium-Base Alloys ...", ASD Technical Documentary Report 63-493, June 1963.

9. J. J. English, "Binary and Ternary Phase Diagrams of Cb, Mo, Ta, and W" DMIC Report 152, April 1961.

10. G. T. Hahn, A. Gilbert, & R. I. Jaffee, "The Effects of Solutes on the Ductile-to-Brittle Transition in Refractory Metals", Refractory Metals and Alloys II, Interscience, New York, 1963.

11. C. S. Wukusick, "Evaluation of Chromium-Ruthenium Alloys", General Electric Report GEMP-362, June 1965.

12. C. S. Wukusick, "The Rhenium Ductilizing Effect", paper presented at AIME Refractory Metals Symposium, French Lick, Indiana, October 1965, (To be published)

13. H. J. Goldschmidt & J. A. Brand, "The Constitution of the Chromium-Niobium-Silicon System", J. Less Comm. Metals 3, (1961) 34.

APPENDIX A

"Kromic" Acid Electrolytic Etchant

H_2O_2	100 ml
KOH	50 ml
H_3PO_4	40 ml
$K_3Fe(CN)_6$	50 g
$H_2C_2O_4$	20 g
$K_4Fe(CN)_6 \cdot 3H_2O$	5 g

Used at 8 $\pm$ 3 volts at a current density of 2 to 3 amps/cm^2.

TABLE 1

ANALYSES OF RAW MATERIALS USED IN ALLOYS OF PHASE A

Element	Purity	Form	Impurities (ppm)									
			O	N	H	C	Fe	Ni	Al	Si	S	Other
Chromium	99.94%	H_2-reduced flake	40	80	<10	80	20	10	5	100	50	-
Chromium	99.997%	Iodide crystal	7	1	.5	9	13	1	.3	10	-	2Ca
Yttrium	99.9%	Sponge	890	8	-	-	20	-	5	50	-	10Ca
Molybdenum	99.9%	Pellets	105	12	-	-	160	61	25	55	-	435W
Tungsten	99.95%	Granules	80	10	-	20	10	20	10	10	-	160Mo
Vanadium	99.9%	Granules	700	50	10	200	-	-	-	-	-	-
Rhenium[a]	99.7%	Powder	1900	150	-	40	Less than 100 ppm total metallics					
Cobalt	99.5%	Shot	140	-	5	100	1100	1700	340	60	60	90Cu
Zirconium[b]	99.8%	Crystal bar	250	20	90	150	20	15	40	50	-	0.9%Hf
Titanium	99.5%	Sheet	1050	130	30	290	800	-	300	-	-	500Sn
Hafnium[b]	99.9%	Crystal bar	160	15	-	70	200	-	15	25	-	1.6%Zr
Columbium	99.8%	EB melted	250	80	-	100	< 100	-	-	<100	-	1000Ta
Tantalum	99.9%	Foil	35	40	5	10	15	5	5	5		25W, 20Cb

[a] Oxygen content reduced to less than 100 ppm by H_2 treatment at 2550°F.

[b] Purity refers to combined Zr and Hf contents.

TABLE 2 COMPOSITIONS OF EXPERIMENTAL CHROMIUM ALLOYS

PHASE A - TASK I

Alloy Designation	Nominal Composition (Atomic %)	Gas Content (ppm) N	O	H	Approx. Analysis [+] (Wt. %) Y	Zr
CI-1	Cr-.1Y	77	120	10	.13	.07
CI-2	Cr-.2Y	104	69	13	.25	.07
CI-3	Cr-.1Y-.05Hf-.03Th	92	25	11	.13	.08
CI-4	Cr-4Mo-.1Y	133	37	8	.15	.06
CI-5	Cr-6Mo-.1Y	72	35	6	.19	.10
CI-6	Cr-8Mo-.1Y	87	19	5	.13	.08
CI-7	Cr-4W-.1Y	89	28	13	.19	< .02
CI-8	Cr-6W-.1Y	89	29	7	.09	.16
CI-9	Cr-4Mo-2W-.1Y	76	22	8	.15	.07
CI-10	Cr-6Mo-2W-.1Y	99	29	6	.15	.07
* CI-11	Cr-4V-.1Y	-	-	-	-	-
* CI-12	Cr-10V-.1Y	-	-	-	-	-
* CI-13	Cr-20V-.1Y	-	-	-	-	-
CI-14	Cr-10V-4Mo-.1Y	86	60	7	.13	.06
CI-15	Cr-10V-4W-.1Y	87	58	7	.02	.08
CI-16	Cr-4Re-.1Y	99	60	5	< .02	< .02
CI-17	Cr-4Co-.1Y	61	41	7	.07	.06
CI-18	Cr-8Co-.1Y	67	86	10	.13	.04
CI-19	Cr-.05Y-4Zr-.2Ti-.4C	81	38	5	< .02	> .40
CI-20	Cr-.1Y-.4Zr-.2Ti-.4C	72	24	6	.07	> .40
CI-21	Cr-.05Y-.3Hf-.3Zr-.4C	74	21	11	< .02	> .40
CI-22	Cr-.05Y-.4Zr-.2Ti-.4B	92	20	7	< .02	> .40
CI-23	Cr-.05Y-.3Hf-.3Zr-.4B	76	19	8	.08	> .40
CI-24	Cr-.05Y-.4Ta-.2Zr-.4B	88	23	8	.08	.25
* CI-25	Cr-4Mo-.05Y-4Zr-.2Ti	-	-	-	-	-
CI-26	Cr-4Mo-.1Y-.4Zr-.2Ti	97	34	12	.08	> .40
CI-27	Cr-4Mo-.1Y-.3Hf-.3Zr	89	18	17	.14	> .40
CI-28	Cr-4Mo-.1Y-.05Hf-.03Th	85	31	6	.03	< .02
CI-29	Cr-4Mo-.05Y-.4Zr-.2Ti-.4C	93	26	11	.05	> .40
CI-30	Cr-4Mo-.1Y-.4Zr-.2Ti-.4C	100	12	13	.15	> .40
CI-31	Cr-4Mo-.05Y-.5Zr-.25Ti-.4C	71	18	13	.05	> .40
CI-32	Cr-4Mo-.05Y-.3Zr-.15Ti-.4C	79	20	9	.09	.28
CI-33	Cr-4Mo-.05Y-.6Ti-.4C	68	16	12	.05	.06
CI-34	Cr-4Mo-.05Y-.6Zr-.4C	86	18	15	.03	> .40
CI-35	Cr-4Mo-.05Y-.6Hf-.4C	13	52	8	.09	.03
CI-36	Cr-4Mo-.05Y-.6Cb-.4C	80	77	5	.05	.06
CI-37	Cr-4Mo-.05Y-.3Hf-.3Zr-.4C	55	43	12	< .02	> .40
CI-38	Cr-4Mo-.05Y-.6Zr-.3Ti-.6C	86	70	16	.05	> .40
CI-39	Cr-4Mo-.05Y-.2Zr-.1Ti-.2C	91	13	12	.07	> .40
CI-40	Cr-4Mo-.05Y-.4Ta-.2Zr-.4C	63	13	12	.05	.40
CI-41	Cr-4Mo-.05Y-.6Ta-.4C	53	36	2	.07	.06
CI-42	Cr-4Mo-.05Y-.4Cb-.2Zr-.4C	46	19	3	.07	.31
CI-43	Cr-4Mo-.2La-.4Cb-.2Zr-.4C	89	134	5	< .02	> .40
CA-2	Cr-35Re	< 10	48	3	-	-

[+] From Quantitative X-Ray Emission

* Dropped From Program

TABLE 3 EXTRUSION DATA - PHASE A ALLOYS

Alloy	Extrusion Temp (°F)	Glass* Lubricant	Extrusion Force (Tons) Upset	Average	Speed (in/sec)
CI-1	2000	7052	150	150	3
CI-2	2000	7052	175	175	2
CI-3	2000	7052	150	130	2.5
CI-4	2700	7740	225	190	2.5
CI-5	2700	7740	250	200	2.5
CI-6	2750	7052	250	250	2.5
CI-7	2750	7740	200	200	2.5
CI-8	2750	7740	200	180	3
CI-9	2750	7740	200	180	3
CI-10	2750	7740	260	225	2
CI-14	2700	7740	225	175	2.5
CI-15	2700	1720	210	210	2.5
CI-16	2750	7052	200	200	4
CI-17	2500	7052	175	160	2.5
CI-18	2500	7052	175	160	2.5
CI-19	2200	7052	175	175	2.5
CI-20	2200	7052	150	125	3
CI-21	2200	7052	135	100	2.5
CI-22	2200	9774	225	200	5
CI-23	2200	8378	175	175	2.5
CI-24	2200	7052	Stalled (temp. too low)		—
CI-24	2400	0010	200	200 (re-run)	4.5
CI-26	2700	7740	235	200	2
CI-27	2750	7052	200	200	2
CI-28	2750	7052	175	175	3
CI-29	2700	7052	200	200	2.5
CI-30	2750	7052	200	200	2
CI-31	2750	7052	175	175	2.5
CI-32	2750	7052	200	200	3
CI-33	2750	7052	225	225	—
CI-34	2750	7052	180	180	3.5
CI-35	2700	7740	235	200	2
CI-36	2750	7052	200	200	4
CI-37	2700	7740	250	220	—
CI-38	2750	7052	200	200	3
CI-39	2750	7052	175	175	2
CI-40	2750	7052	175	175	4
CI-41	2750	7052	225	225	2.5
CI-42	2750	7052	225	225	2.5
CI-43	2750	7052	260	260	—

* Corning Designation

TABLE 4 EFFECT OF PROCESSING ON THE MICROHARDNESS OF PHASE A CHROMIUM ALLOYS

Alloy	Nominal Composition (Atomic %)	Diamond Pyramid Hardness (kg/mm^2)+ Cast	Extruded	Swaged	Swaging Temp. (°F)
CI-1	Cr-.1Y	101	156	177	1900
CI-2	Cr-.2Y	111	165	172	1900
CI-3	Cr-.1Y-.05Hf-.03Th	115	142	221	1900
CI-4	Cr-4Mo-.1Y	251	268	325	2100
CI-5	Cr-6Mo-.1Y	330	306	332 *	2250
CI-6	Cr-8Mo-.1Y	345	353	- *	-
CI-7	Cr-4W-.1Y	297	299	358	2250
CI-8	Cr-6W-.1Y	307	371	- *	2300
CI-9	Cr-4Mo-2W-.1Y	339	332	- *	-
CI-10	Cr-6Mo-2W-.1Y	378	333	- *	2300
CI-14	Cr-10V-4Mo-.1Y	310	401	- *	2200
CI-15	Cr-10V-4W-.1Y	313	349	- *	-
CI-16	Cr-4Re-.1Y	183	240	274	2250
CI-17	Cr-4Co-.1Y	330	336	353	2200
CI-18	Cr-8Co-.1Y	493	524	- *	-
CI-19	Cr-.05Y-.4Zr-.2Ti-.4C	137	166	191	2000
CI-20	Cr-.1Y-.4Zr-.2Ti-.4C	128	136	188	2000
CI-21	Cr-.05Y-.3Hf-.3Zr-.4C	134	146	175	2000
CI-22	Cr-.05Y-.4Zr-.2Ti-.4B	122	157	190	2000
CI-23	Cr-.05Y-.3Hf-.3Zr-.4B	116	150	206	2000
CI-24	Cr-.05Y-.4Ta-.2Zr-.4B	158	198	206	2200
CI-26	Cr-4Mo-.1Y-.4Zr-.2Ti	279	283	296	2200
CI-27	Cr-4Mo-.1Y-.3Hf-.3Zr	241	296	-	2200
CI-28	Cr-4Mo-.1Y-.05Hf-.03Th	283	268	-	2200
CI-29	Cr-4Mo-.05Y-.4Zr-.2Ti-.4C	260	265	-	2200
CI-30	Cr-4Mo-.1Y-.4Zr-.2Ti-.4C	274	280	293	2250
CI-31	Cr-4Mo-.05Y-.5Zr-.25Ti-.4C	236	286	345	2200
CI-32	Cr-4Mo-.05Y-.3Zr-.15Ti-.4C	261	289	-	2250
CI-33	Cr-4Mo-.05Y-.6Ti-.4C	287	327	369	2200
CI-34	Cr-4Mo-.05Y-.6Zr-.4C	266	311	311	2200
CI-35	Cr-4Mo-.05Y-.6Hf-.4C	292	274	316	2200
CI-36	Cr-4Mo-.05Y-.6Cb-.4C	274	322	376	2250
CI-37	Cr-4Mo-.05Y-.3Hf-.3Zr-.4C	296	283	316	2200
CI-38	Cr-4Mo-.05Y-.6Zr-3Ti-.6C	283	292	356	2250
CI-39	Cr-4Mo-.05Y-.2Zr-.1Ti-.2C	287	274	306	2200
CI-40	Cr-4Mo-.05Y-.4Ta-.2Zr-.4C	260	277	-	2250
CI-41	Cr-4Mo-.05Y-.6Ta-.4C	280	333	363	2250
CI-42	Cr-4Mo-.05Y-.4Cb-.2Zr-.4C	279	311	-	2300
CI-43	Cr-4Mo-.2La-.4Cb-.2Zr-.4C	262	333	-	2350
CA-2	Cr-35Re	330	-	437	2200

+ 2.5 Kilogram load.

* Impact extruded prior to final swaging trials.

TABLE 5

EFFECTS OF POST-WORK ANNEALING

ON TENSILE BEHAVIOR OF REPRESENTATIVE CHROMIUM ALLOYS AT LOW TEMPERATURES

Alloy	Nominal Comp. (At. %)*	1-Hr. Anneal Temp °F	Tensile Properties at: - 50°F UTS ksi	- 50°F RA %	75°F UTS ksi	75°F RA %	200°F UTS ksi	200°F RA %	400°F UTS ksi	400°F RA %	600°F UTS ksi	600°F RA %
CI-1	.10Y	2000	-	-	38.8	1.5	45.4	78.3	-	-	-	-
		2400	-	-	32.7	0	43.9	69.8	-	-	-	-
CI-4	4Mo-.10Y	1800	-	-	-	-	86.1	1.6	94.0	26.9	-	-
		2000	-	-	-	-	78.3	1.7	90.6	29.9	-	-
		2400	-	-	-	-	-	-	72.5	3.4	95.2	53.5
CI-19	.05Y-ZTC	1800	-	-	-	-	72.0	61.1	58.0	71.6	-	-
		2000	-	-	59.4	8.2	64.1	61.6	54.9	73.0	-	-
		2400	72.5	0	59.2	11.7	-	-	-	-	-	-
CI-20	.10Y-ZTC	2000	71.9	0.5	57.6	24.6	-	-	-	-	-	-
CI-21	.05Y-HZC	1800	-	-	-	-	66.0	57.6	67.0	70.0	-	-
		2000	67.7	0.8	71.5	24.2	63.5	64.8	54.7	70.7	-	-
		2400	-	-	52.1	7.9	50.7	37.1	-	-	-	-
CI-30	4Mo-.10Y-ZTC	2000	-	-	-	-	-	-	68.6	1.8	69.6	1.5
CI-37	4Mo-.05Y-HZC	1800	-	-	-	-	-	-	95.8	1.6	99.5	48.8
		2000	-	-	-	-	-	-	104.0	5.7	104.5	48.0
		2400	-	-	-	-	-	-	77.4	3.9	113.0	5.5

*Balance Cr, ZTC = .4Zr-.2Ti-.4C, HZC = .3Hf-.3Zr-.4C

TABLE 6

TENSILE PROPERTIES OF WROUGHT CHROMIUM ALLOYS

AFTER ONE-HOUR ANNEALING AT 2000°F ($\dot{\varepsilon}$ = .03 PER MINUTE)

Alloy	Nominal Composition (Atomic %)	Test Temp °F	UTS (ksi)	.2% Offset (ksi)	Elong. %	RA %
CI-1	Cr-.10Y	75	38.0	38.0	1.5	1.5
		200	45.4	28.1	59.2	78.3
		1900	12.4	8.4	67.1	96.5
		2400	5.2	3.4	58.2	96.0
CI-2	Cr-.20Y	75	42.9	42.0	0.4	1.7
		1900	9.3	5.8	63.1	95.1
		2400	4.2	3.4	69.4	95.6
CI-3	Cr-.10Y-.05Hf-.03Th	75	43.9	32.8	5.9	6.4
		1900	19.9	19.4	22.3	87.7
		2400	5.5	4.1	68.5	78.2
CI-4	Cr-4Mo-.10Y	200	78.3	73.3	1.0	1.7
		400	90.6	69.4	18.4	29.9
		600	88.5	67.0	26.7	44.0
		1900	46.4	37.2	16.8	48.2
		2400	17.6	16.5	31.9	32.8
CI-5	Cr-6Mo-.10Y	2400	24.0	22.8	14.2	15.4
CI-7	Cr-4W-.10Y	1900	63.6	58.9	20.7	74.3
		2400	24.3	22.7	19.5	24.5
CI-8	Cr-6W-.10Y	1900	81.0	73.2	19.3	71.5
		2400	30.1	28.5	48.6	66.0
CI-10	Cr-6Mo-2W-.10Y	2400	29.2	28.7	28.1	30.5
CI-14	Cr-10V-4Mo-.10Y	1900	68.9	59.7	22.0	75.1
		2400	22.8	22.0	17.3	22.4
CI-17	Cr-4Co-.10Y	200	67.9	> 67.9	0.1	0
		1900	21.7	20.5	75.7	81.5
		2400	4.9	4.1	128.0	90.0
CI-19	Cr-.05Y-.4Zr-.2Ti-.4C	-50	72.5	> 72.5	0	0
		0	63.8	50.2	3.1	3.3
		75	59.4	38.6	8.0	8.2
		200	64.1	34.6	39.5	61.6

TABLE 6

(Continued)

Alloy	Nominal Composition (Atomic %)	Test Temp °F	UTS (ksi)	.2% Offset (ksi)	Elong. %	RA %
CI-19	Cr-.05Y-.4Zr-.2Ti-.4C	400	54.9	30.3	43.5	73.0
		1900	21.7	19.2	30.0	87.5
		2400	7.9	6.3	55.8	95.5
CI-20	Cr-.10Y-.4Zr-.2Ti-.4C	-50	71.9	70.8	0.5	0.5
		75	57.6	42.2	22.7	24.6
		1900	15.1	8.7	48.8	72.7
		2400	5.9	4.5	59.0	63.2
CI-21	Cr-.05Y-.3Hf-.3Zr-.4C	-50	67.7	67.0	0.8	0.8
		75	71.5	45.5	21.3	24.2
		200	63.5	34.4	57.2	64.8
		400	54.7	33.1	60.8	70.7
		1900	36.5	35.0	30.2	86.5
		2400	5.9	5.0	94.2	91.5
CI-22	Cr-.05Y-.4Zr-.2Ti-.4B	75	82.9	56.9	12.9	12.9
		1900	35.7	33.4	17.3	79.7
		2400	8.0	6.5	91.5	97.5
CI-23	Cr-.05Y-.3Hf-.3Zr-.4B	75	67.0	63.5	1.5	1.8
		1900	34.8	33.0	16.7	73.7
		2400	8.9	7.8	82.0	95.0
CI-26	Cr-4Mo-.10Y-.4Zr-2Ti	400	36.9	> 36.9	0	0
		1900	54.9	44.8	22.8	61.9
		2400	20.1	19.5	40.5	43.1
CI-27	Cr-4Mo-.05Y-.3Hf-.3Zr	1900	52.8	49.5	18.0	64.2
		2400	18.3	16.6	50.6	62.7
CI-28	Cr-4Mo-.10Y-.05Hf-.03Th	1900	49.7	42.2	17.4	49.5
		2400	18.1	17.4	21.2	24.8
CI-29	Cr-4Mo-.05Y-.4Zr-.2Ti-.4C	1900	56.4	52.0	27.8	72.7
		2400	20.9	20.7	19.6	29.8
CI-30	Cr-4Mo-.10Y-.4Zr-.2Ti-.4C	400	68.6	59.7	1.6	1.8
		600	69.9	59.6	1.5	1.5
		1900	47.8	41.3	14.9	29.8
		2400	18.8	15.9	23.9	31.8
CI-31	Cr-4Mo-.05Y-.5Zr-.25Ti-.4C	400	51.2	> 51.2	0	0
		1900	46.7	32.8	23.9	45.8
		2400	19.8	19.1	18.5	23.4

TABLE 6

(Continued)

Alloy	Nominal Composition (Atomic %)	Test Temp °F	UTS (ksi)	.2% Offset (ksi)	Elong %	RA %
CI-32	Cr-4Mo-.05Y-.3Zr-.15Ti-.4C	1900	56.6	49.8	25.8	82.0
		2400	17.1	14.9	46.5	90.5
CI-35	Cr-4Mo-.05Y-.6Hf-.4C	400	90.5	74.4	2.3	3.2
		1900	58.2	54.2	19.6	59.2
		2400	19.3	18.7	37.9	38.1
CI-37	Cr-4Mo-.05Y-.3Hf-.3Zr-.4C	400	104.0	84.7	4.1	5.7
		600	104.5	77.2	28.2	48.0
		1900	61.0	57.2	26.2	71.7
		2100	39.2	31.9	41.7	75.7
		2300	23.5	21.0	56.4	56.7
		2400	20.7	19.7	46.2	50.2
CA-2	Cr-35Re	1900	69.7	63.2	16.0	28.8
		2400	22.3	17.0	38.8	39.1

TABLE 7

Cr-W-V ALLOY COMPOSITIONS AND METALLOGRAPHIC DATA

Alloy Composition (At. %)*		2900°F, 2 Hrs.		+ 1800°F, 200 Hrs.	
W	V	DPH	Structure	DPH	Structure
4.9	--	313	Single Phase	329	Single Phase
7.8	--	321	"	321	"
10.0	--	417	"	429	2 - Phase
5.1	5.1	358	"	337	Single Phase
4.8	9.6	358	"	346	2 - Phase
7.3	4.7	387	"	405	Single Phase
7.8	10.4	444	"	418	2 - Phase
7.6	15.5	417	"	438	"
10.1	10.1	453	"	459	"
10.3	15.6	458	"	479	"
10.1	20.3	448	"	482	"

* Calculated from charge weights and weight changes during melting.

TABLE 8

COMPOSITIONS AND METALLOGRAPHIC OBSERVATIONS IN Cr-Re-Co ALLOYS

Composition (At. %)		Metallographic Observations			
		2750°F, 2 Hrs.		+ 1650°F, 100 Hrs.	
Co	Re	Structure	DPH *	Structure	DPH *
5.75	30.2	2 - Phase	477	2 - Phase	487
2.5	25.6	Single Phase	365	Single Phase	371
4.9	24.8	" "	439	Slight Precipitate	439
5.2	20.4	" "	465	" "	435
7.5	18.9	" "	524	" "	515
5.1	15.3	" "	453	Single Phase	430
10.4	14.2	" "	564	Slight Precipitate	571

* Diamond Pyramid Hardness, 1 Kg Load

TABLE 9

EFFECTS OF SOLUTES FROM GROUPS IV A AND V A
ON THE AIR OXIDATION OF Cr-Y-C ALLOYS

Nominal Composition (At. %)	100-Hour Weight Gain (mg/cm^2) at 2100°F[a]					
	M = Ti	Zr	Hf	V	Cb	Ta
Cr-.5M	18.9	13.3	16.1	-	22.3	19.3
Cr-.5M-.1Y	2.7	1.4	2.8	12.8	12.2	14.2
Cr-.5M-.2Y	2.3	2.5	1.9	13.1	11.3	11.4
Cr-.5M-.4C	14.2	4.6	8.2	-	20.8	17.8
Cr-.5M-.4C-.1Y	4.6	3.0	5.7	3.0	18.1	12.9
Cr-.5M-.4C-.2Y	4.8	2.9	4.0	1.8	10.0	13.3
Cr-1M-.4C	11.9	3.7	6.6	10.2	33.1	-
Cr-1M-.4C-.1Y	2.5	3.0	2.3	8.4	24.5	13.9
Cr-1M-.4C-.2Y	2.3	2.2	3.4	2.3	12.5	-

[a]The 100-hour weight gains of unalloyed Cr and Cr-.1Y are 12.7 and 2.0 mg/cm^2, respectively, at 2100°F.

TABLE 10

LOW-TEMPERATURE BEND PROPERTIES OF SELECTED CARBIDE-STRENGTHENED CHROMIUM ALLOYS AND EFFECTS OF AIR OXIDATION

Nominal Composition (At. %)	Rolled + Annealed			1500°F-100 Hr.-Air		2100°F-100 Hr.-Air	
	DPH (kg/mm^2)[a]	DBTT (°F)[b]	400°F σ_D (ksi)[c]	DBTT (°F)	800°F σ_D (ksi)	DBTT (°F)	800°F σ_D (ksi)
Cr-.1Y	138	-50	18.1	< 75	11.4	100	14.2
Cr-1Ti-.4C	216	200	79.0	800	74.3	> 800	47.7
Cr-1Ti-.4C-.1Y	217	200	72.1	500	65.5	600	49.4
Cr-1Zr-.4C	161	75	48.6	400	41.7	800	37.4
Cr-1Zr-.4C-.1Y	152	0	47.1	200	58.8	300	35.7
Cr-1Zr-.4C-.2Y	156	75	55.3	400	41.0	200	27.5
Cr-1Hf-.4C-.1Y	172	150	42.4	200	59.7	400	25.8
Cr-1Hf-.4C-.2Y	160	100	50.4	-	-	200	31.5
Cr-1V-.4C	140	75	19.0	-	-	> 800	15.0
Cr-1V-.4C-.1Y	142	-50	17.3	200	24.7	> 800	26.1
Cr-1V-.4C-.2Y	149	100	28.5	-	-	Broke in handling	
Cr-1Cb-.4C	215	300	74.1	> 800	69.5	Broke in handling	
Cr-1Cb-.4C-.1Y	199	200	77.2	800	80.1	> 800	68.6
Cr-1Ta-.4C-.1Y	224	300	82.9	-	-	> 800	70.5

a) Diamond pyramid hardness, 100 gram load.

b) Ductile-brittle transition temperature based on 15° deflection in 4T bend tests at a ram speed of .05 ipm.

c) σ_D denotes fiber stress at deviation from linearity on load-time curves at indicated temperatures.

TABLE 11

HARDNESS AND OXIDATION BEHAVIOR OF ALLOYS IN THE Cr-Y-Cb-Si SYSTEM

Alloy (At. %)			Cast DPH	SA DPH*	Aged DPH (kg/mm^2)		100-Hr. Air Oxidation At 2100°F**	
Y	Cb	Si	(kg/mm^2)	(kg/mm^2)	1800°F/25 hr.	2200°F/5 hr.	Wt. Change (mg/cm^2)	Nitride (Mils)
0.1	-	-	101	-	-	-	2.0	0
0.1	0.5	-	170	145	165	160	17.4	1.5
0.1	1.0	-	219	190	198	207	29.1	2.5
0.1	1.5	-	262	231	251	274	44.4	7.5
-	1.5	-	371	322	322	279	- 71.4	13.5
0.1	3.0	-	363	327	322	287	72.5	15.0
0.1	4.5	-	405	350	356	405	117.0	17.0
0.1	-	1.0	131	221	137	145	5.3	1.0
0.1	-	2.0	160	243	162	160	10.0	0.7
-	-	4.0	247	283	251	227	17.3	2.0
0.1	-	4.0	240	311	243	236	12.1	1.5
0.1	1.5	1.0	296	279	254	240	40.0	6.0
0.1	3.0	2.0	383	327	311	296	46.2	16.0
0.1	4.5	4.0	441	383	344	397	53.5	12.0

*Solution annealed at 2600°F, one hour
All Diamond Pyramid Hardnesses at 2.5 kg load

**Oxidation tests conducted on samples forged 60-70% at 2300°F

TABLE 12 AIR OXIDATION OF DISPERSED-CARBIDE ALLOYS WITH La, Pr AND MM

Nominal Comp.[a] (At. %)	Temp. (°F)	Weight Gain (mg/cm²) Total	Net	DPH, 1Kg Edge	Core	Comments[b]
Cr-ZTC	1500	0.31	0.31	283	249	
	2100	2.5	-3.2	1332	252	Thick surface nitrides
	2400	7.5	-6.7	1226	202	at 2100° and 2400°F.
Cr-ZTC-.2La	1500	0.30	0.30	251	200	
	2100	0.20	0.20	247	178	Little or no nitriding.
	2400	0.40	-0.6	225	179	
Cr-ZTC-.5La	1500	0.26	0.26	270	206	
	2100	0.75	0.75	227	212	No nitriding at any T.
	2400	0.70	0.70	230	199	
Cr-ZTC-.2Pr	1500	0.27	0.27	281	224	
	2100	0.86	0.86	276	254	Small am't. intergranular
	2400	1.3	0.80	233	179	nitride at 2100° and 2400°F.
Cr-ZTC-.5Pr	1500	0.48	0.48	322	239	
	2100	1.5	1.5	247	196	No nitriding.
	2400	1.9	1.9	227	170	
Cr-ZTC-.2MM	1500	0.39	0.39	278	241	
	2100	1.5	1.5	254	178	Some IG nitride at 2100°F,
	2400	1.9	1.9	251	186	thin layer at 2400°F.
Cr-ZTC-.5MM	1500	0.67	0.67	281	236	
	2100	1.2	1.2	264	199	Small am't IG nitride.
	2400	2.0	2.0	221	192	
Cr-CbC-.2La	1500	0.54	0.54	297	297	
	2100	7.1	4.3	630	189	Extensive nitriding.
	2400	67.0 [c]	-20.0	1560	1452	
Cr-CbC-.5La	1500	0.04	0.04	258	236	
	2100	0	0	247	221	Little or no nitriding.
	2400	0.9	0.5	260	192	
Cr-CbC-.2Pr	1500	0.22	0.22	251	251	
	2100	5.2	5.2	268	230	Extensive nitriding.
	2400	6.7	-23.0	1750	199	
Cr-CbC-.2MM	1500	0.92	0.92	281	289	
	2100	3.1	1.9	1081	192	Extensive nitriding.
	2400	71.5 [c]	-29.2	1505	292	
Cr-TiC-.2La	1500	0.78	0.78	281	233	Little or no nitride;
	2100	6.7	6.7	258	198	thick irregular oxide
	2400	3.6	3.2	251	184	with internal stringers.
Cr-.2La	1500	0.10	0.10	196	198	
	2100	0.98	0.98	183	189	No nitriding or incipient
	2400	1.3	1.3	197	160	melting.
Cr-.5La	1500	0.26	0.26	160	201	
	2100	0.03	0.03	138	150	No nitriding, but incipient
	2400	4.5	-1.7	143	137	melting at 2100° and 2400°F.

a) ZTC = .4Zr-.2Ti-.4C
CbC = .6Cb-.4C
MM = mischmetal

b) No nitriding at 1500°F in any alloy.

c) Specimen badly cracked.

A. CI-1 (Cr-.1Y)

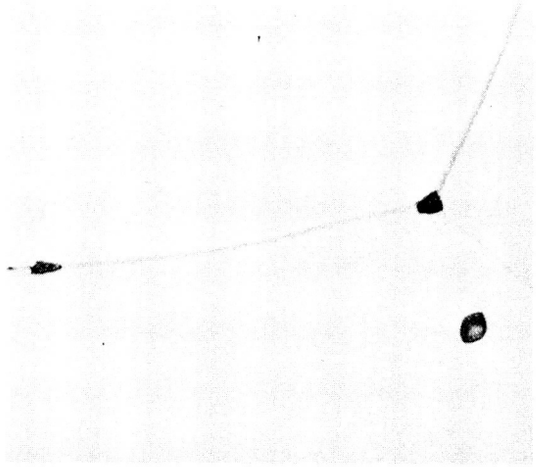

E6024 1000X

B. CI-16 (Cr-4Re-.1Y)

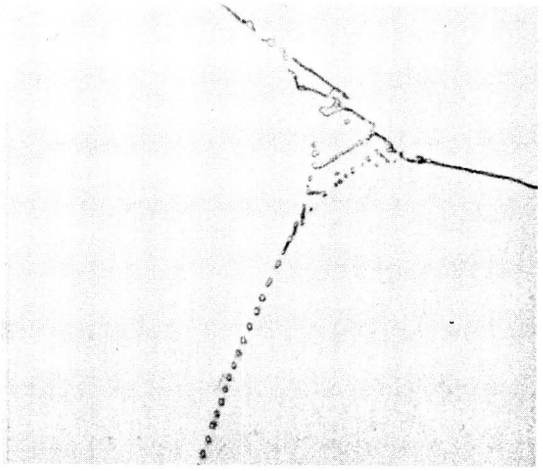

E6647 1000X

C. CI-19 (Cr-.05Y-ZTC)

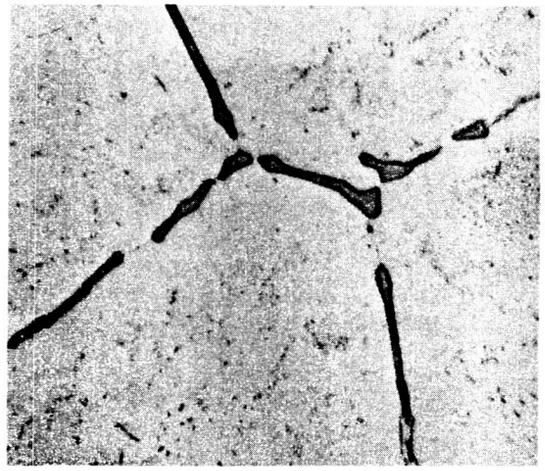

E5054 1000X

D. CI-21 (Cr-.05Y-HZC)

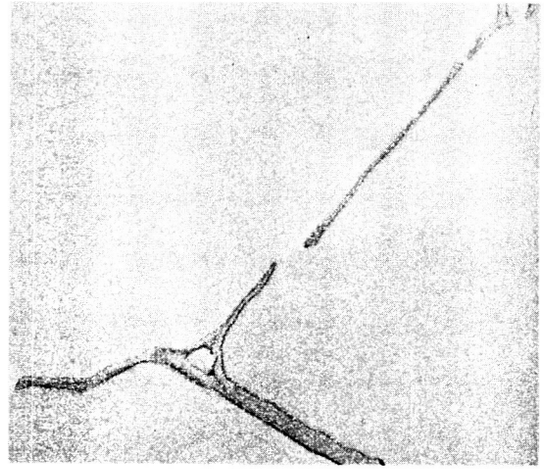

E5162 1000X

E. CI-33 (Cr-.05Y-TiC)

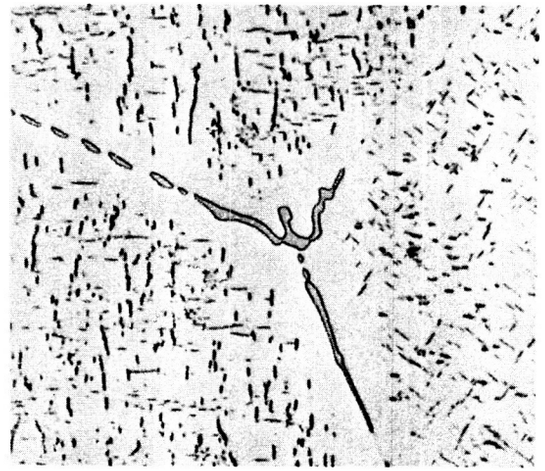

F1089 1000X

F. CI-36 (Cr-.05Y-CbC)

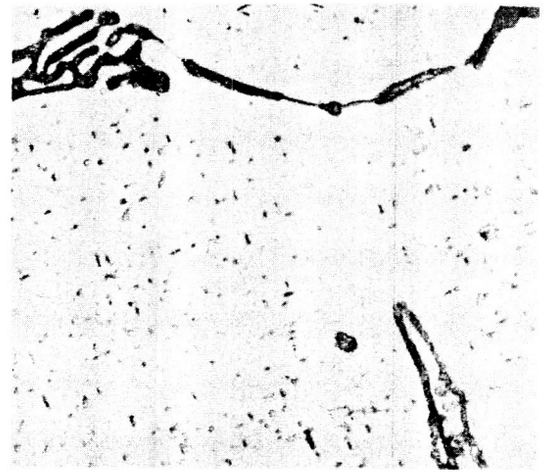

F1091 1000X

Figure 1. Cast microstructures of induction-melted chromium alloys. Etched Kromic acid.

A. CI-1 (Cr-.10Y)

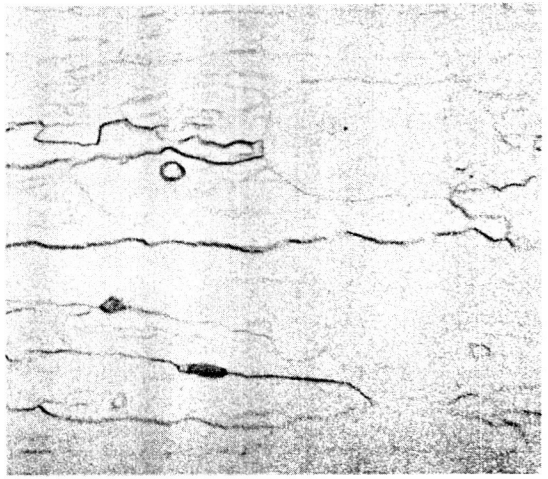

F1493 1000X

C. CI-19 (Cr-.05Y-ZTC)

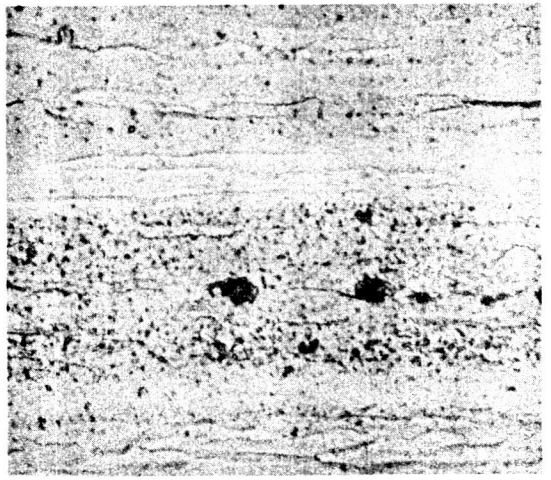

E5306 1000X

E. CI-33 (Cr-.05Y-TiC)

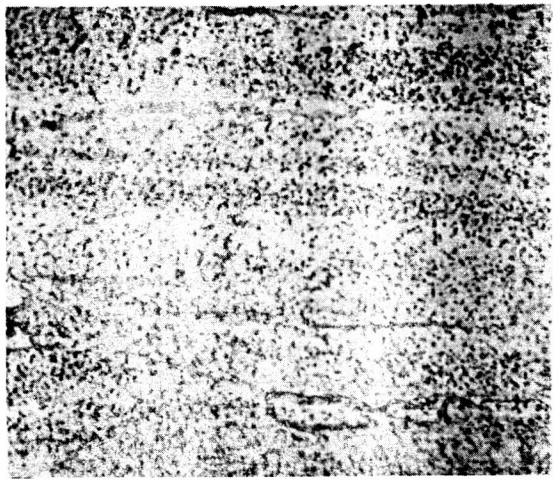

F2332 1000X

B. CA-2 (Cr-35Re)

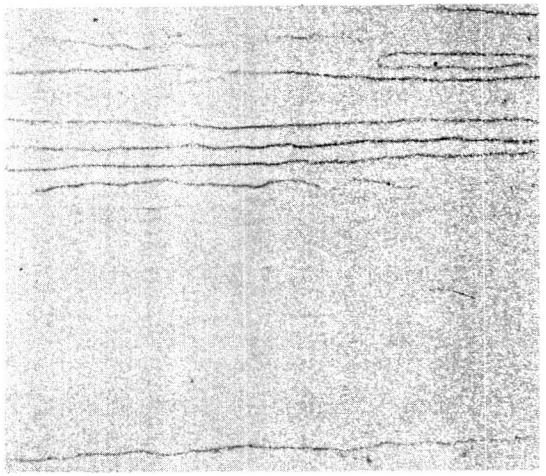

F1476 1000X

D. CI-21 (Cr-.05Y-HZC)

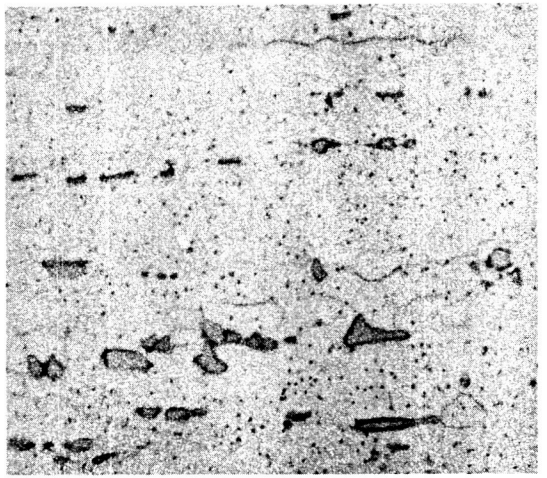

E5734 1000X

F. CI-36 (Cr-.05Y-CbC)

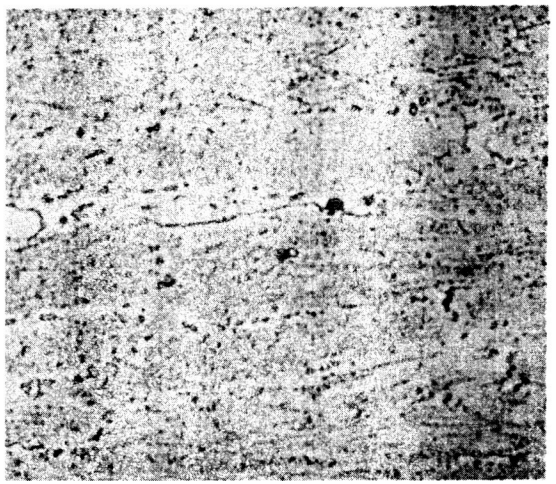

F2334 1000X

Figure 2. Microstructures of swaged chromium alloys. Etched in Kromic acid.

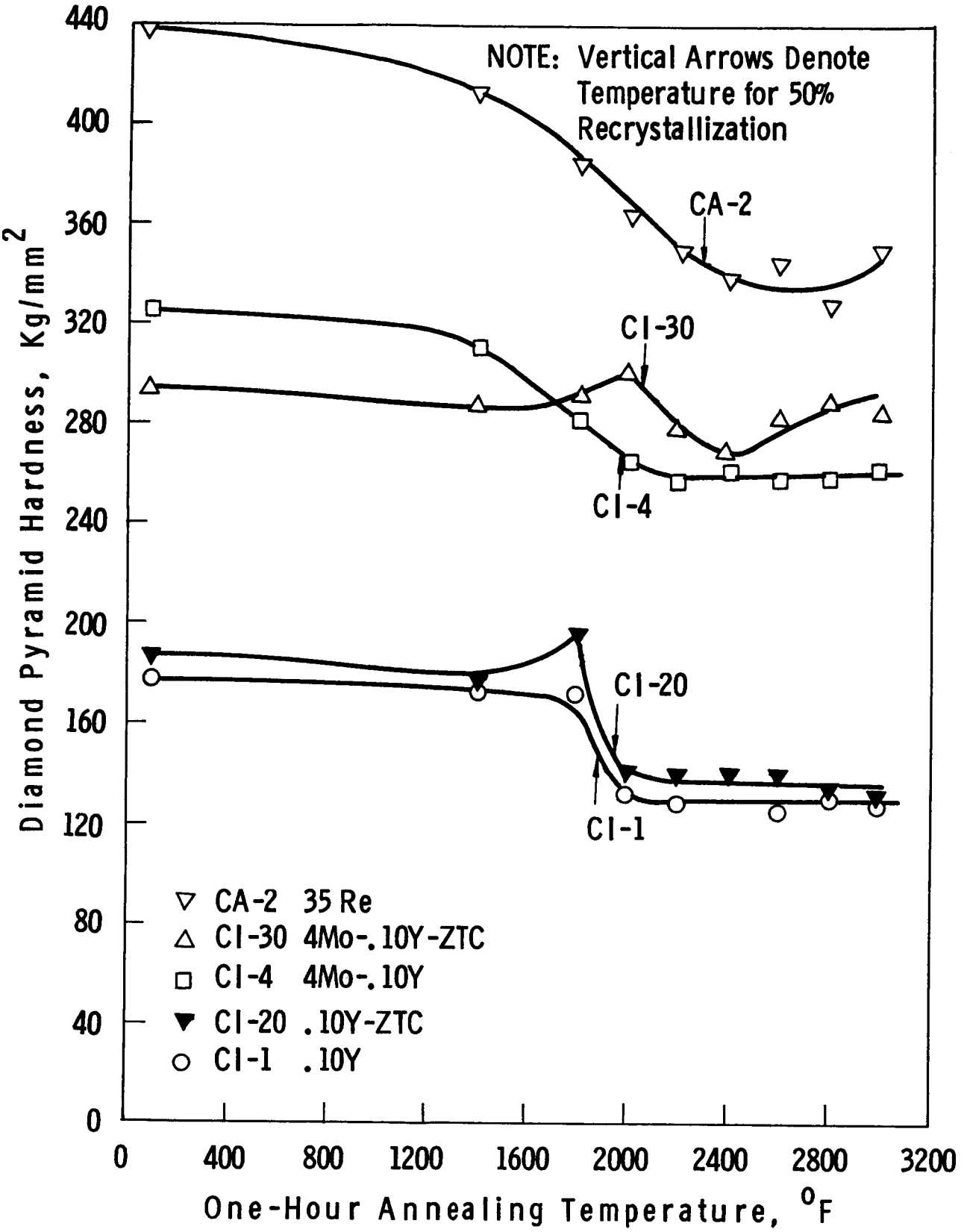

Figure 3. Effect of annealing on the microhardness and recrystallization of representative chromium alloys.

E6028 1000X

A. As Swaged

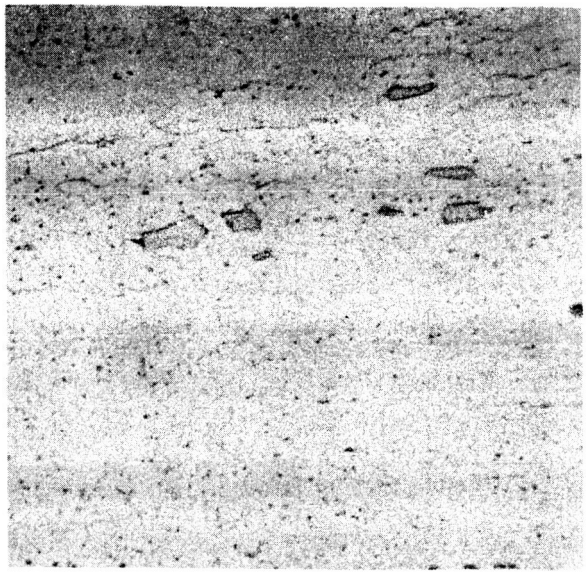

E6029 1000X

B. A + 2000°F, One Hour

E6032 1000X

C. A + 2200°F, One Hour

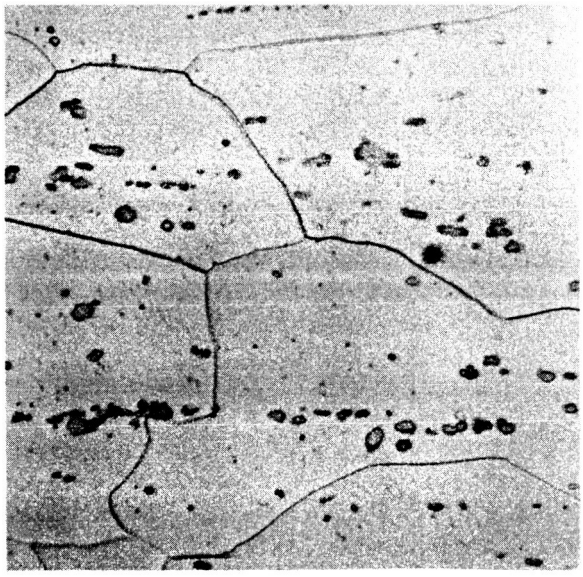

F722 1000X

D. A + 2400°F, One Hour

Figure 4. Effect of indicated annealing treatments on the distribution of carbides in alloy CI-37 (Cr-4Mo-.05Y-HZC). Etched in Kromic acid.

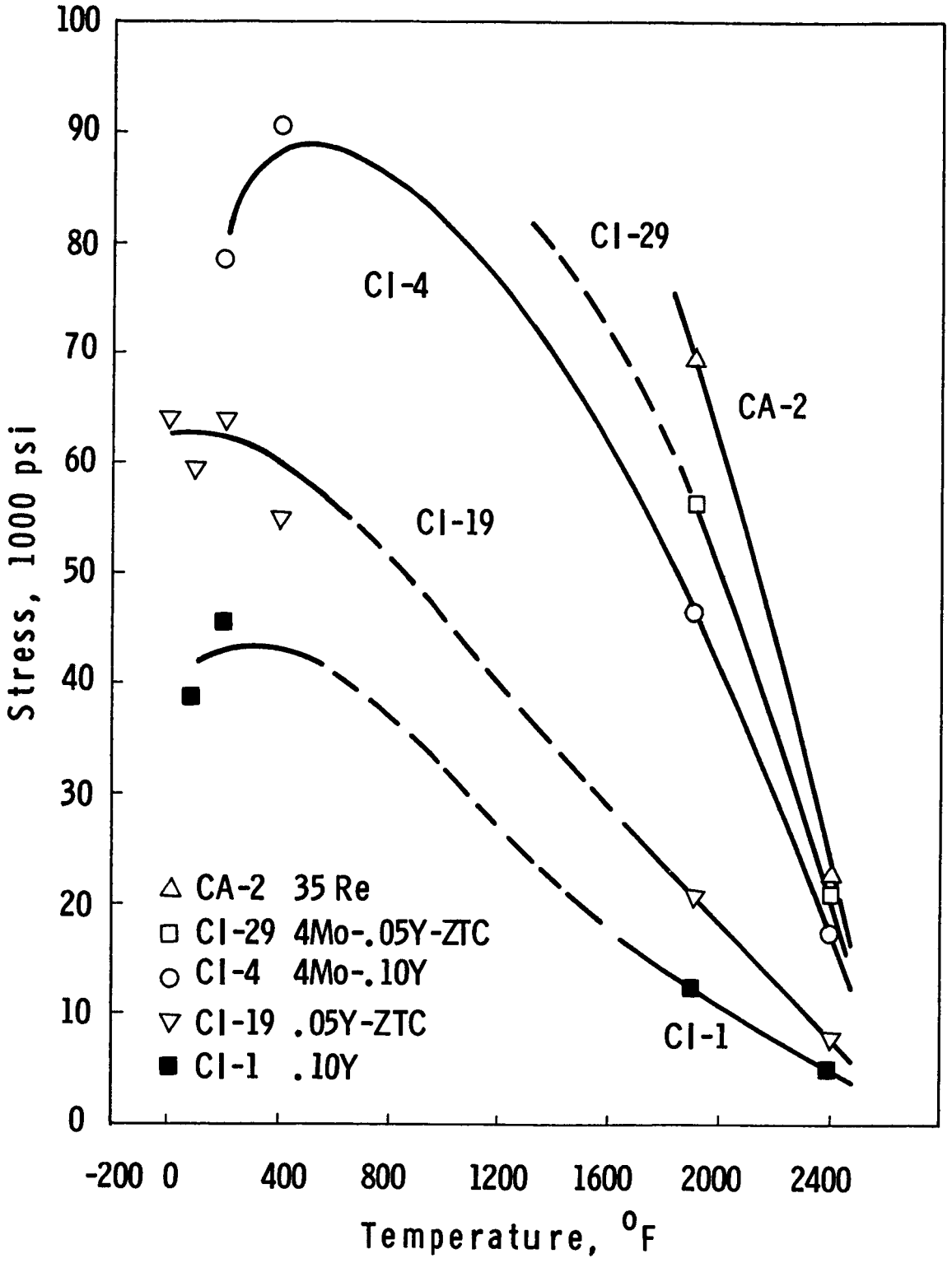

Figure 5. Tensile strengths of representative alloys after one-hour annealing at 2000°F. ($\dot{\epsilon}$ = .03 Min^{-1}).

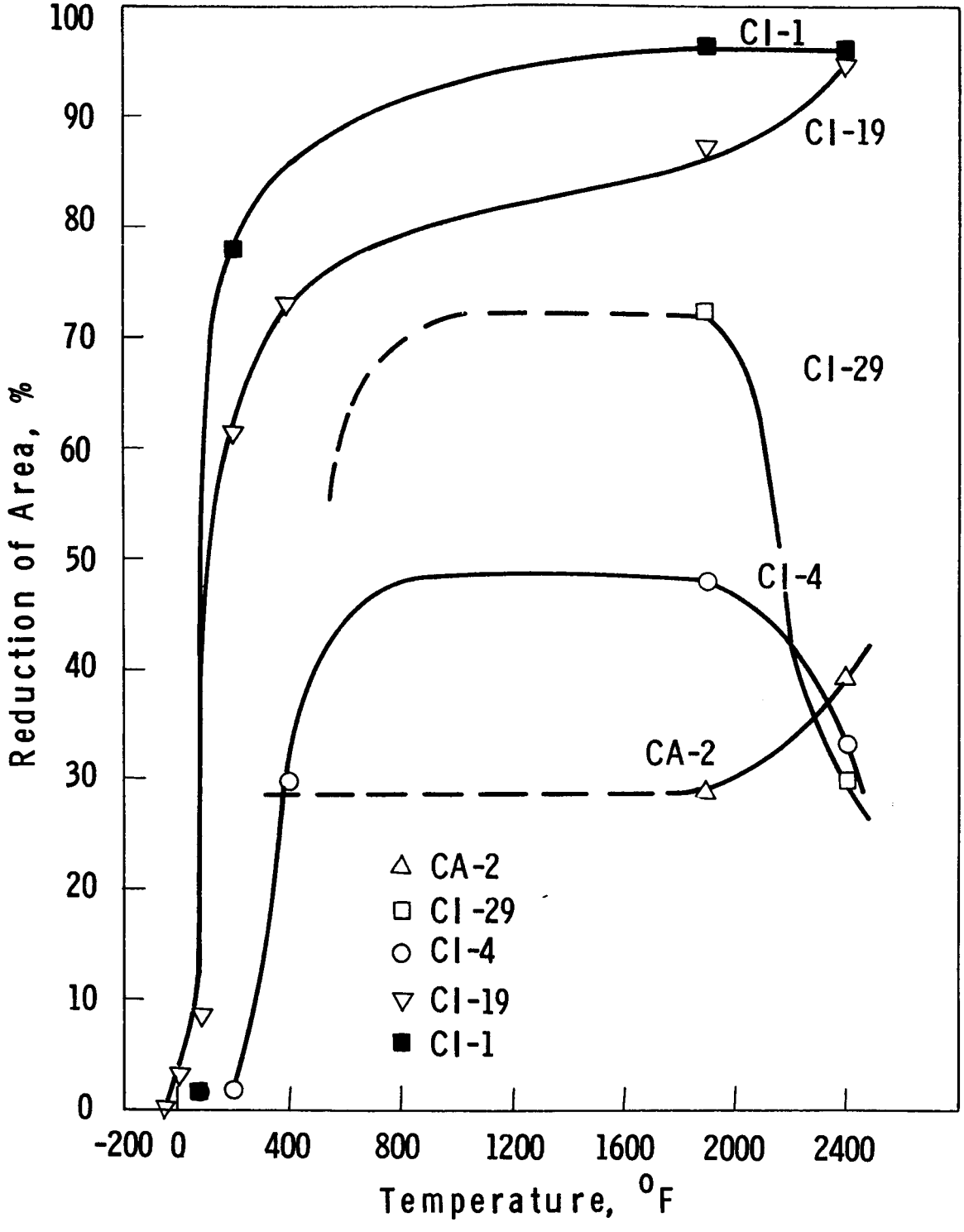

Figure 6. Tensile ductility of representative alloys after one-hour annealing at 2000°F (See Figure 5 for compositions).

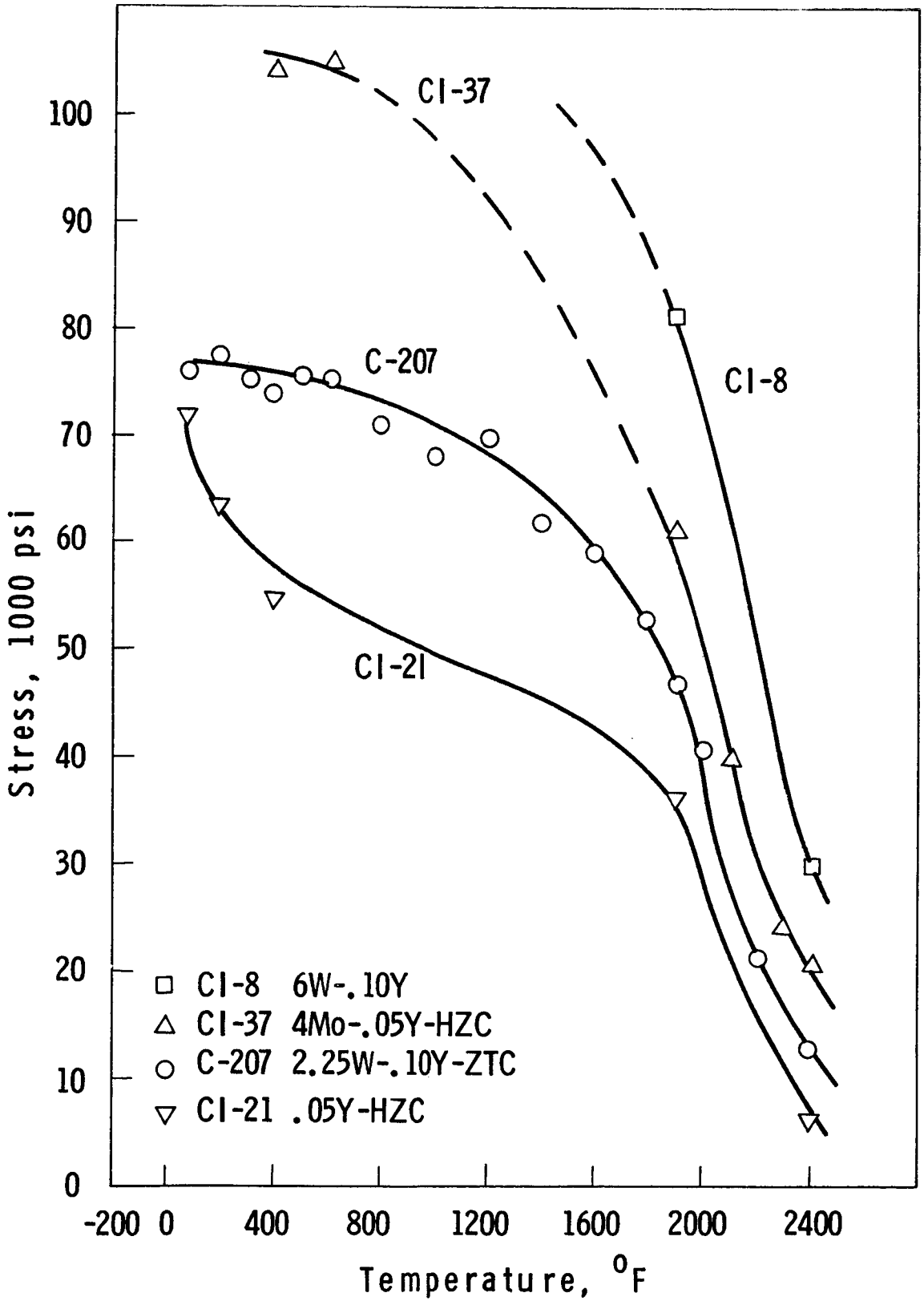

Figure 7. Tensile strengths of strongest alloys of each general type after 2000°F - 1 hour annealing ($\dot{\epsilon}$ = .03 min^{-1}).

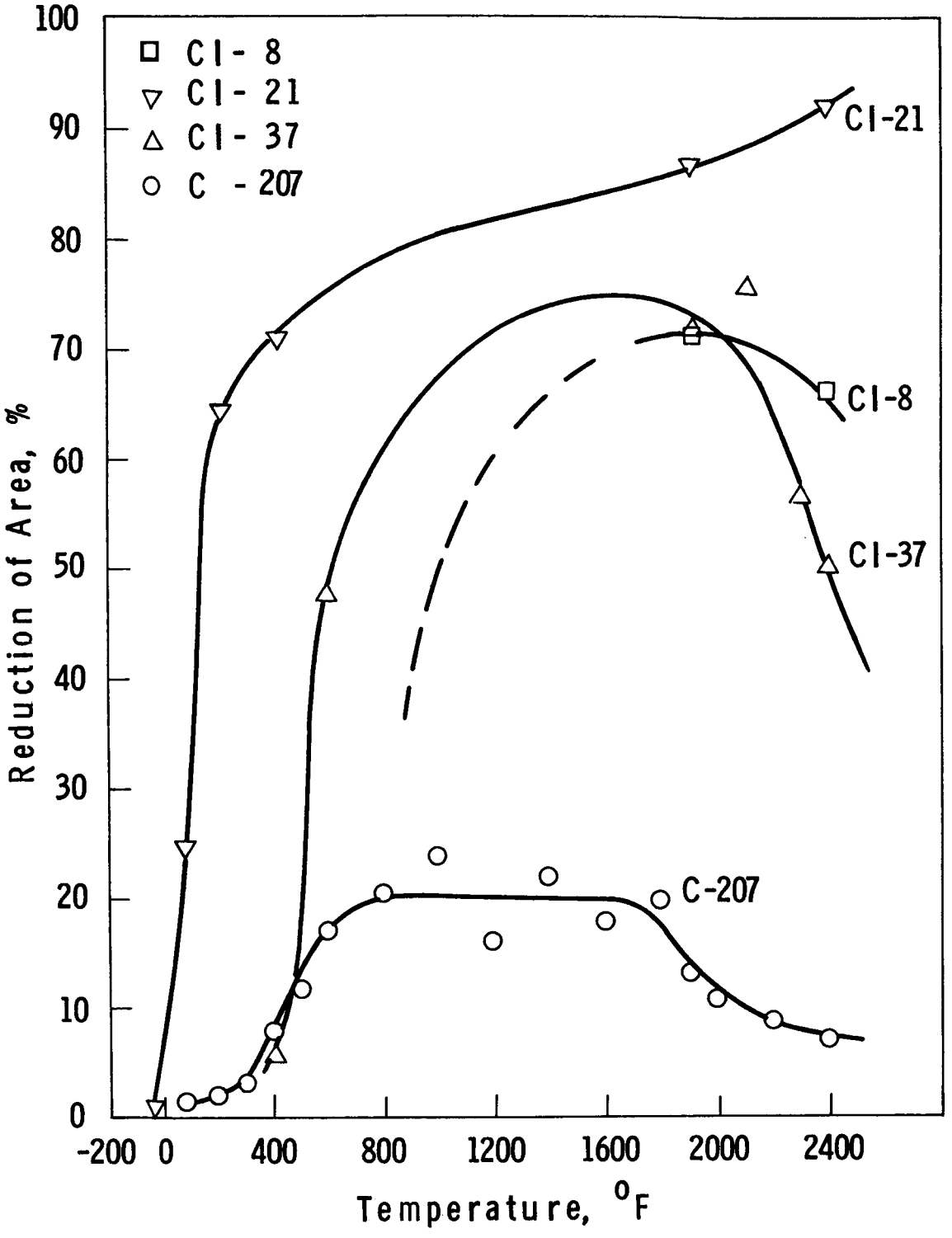

Figure 8. Tensile ductility of strongest alloys of each general type after 2000°F - 1 hour annealing (See Figure 7 for compositions).

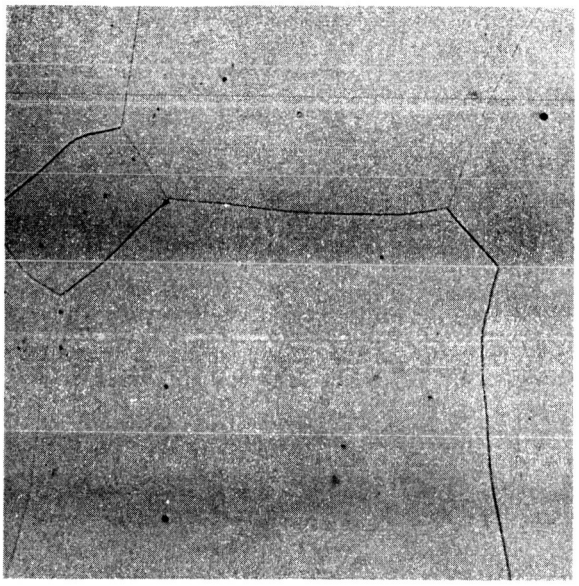

A. Cr-5.1W-5.1V 250X

B. Cr-4.8W-9.6V 250X

C. Cr-10.3W-15.6V 250X

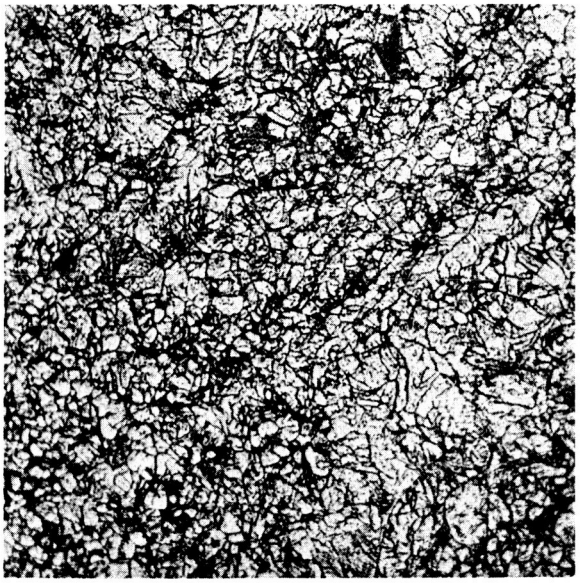

D. Cr-10.1W-20.3V 250X

Figure 9. Microstructures of Cr-W-V alloys aged 200 hours at 1800°F. Etched 10% oxalic acid.

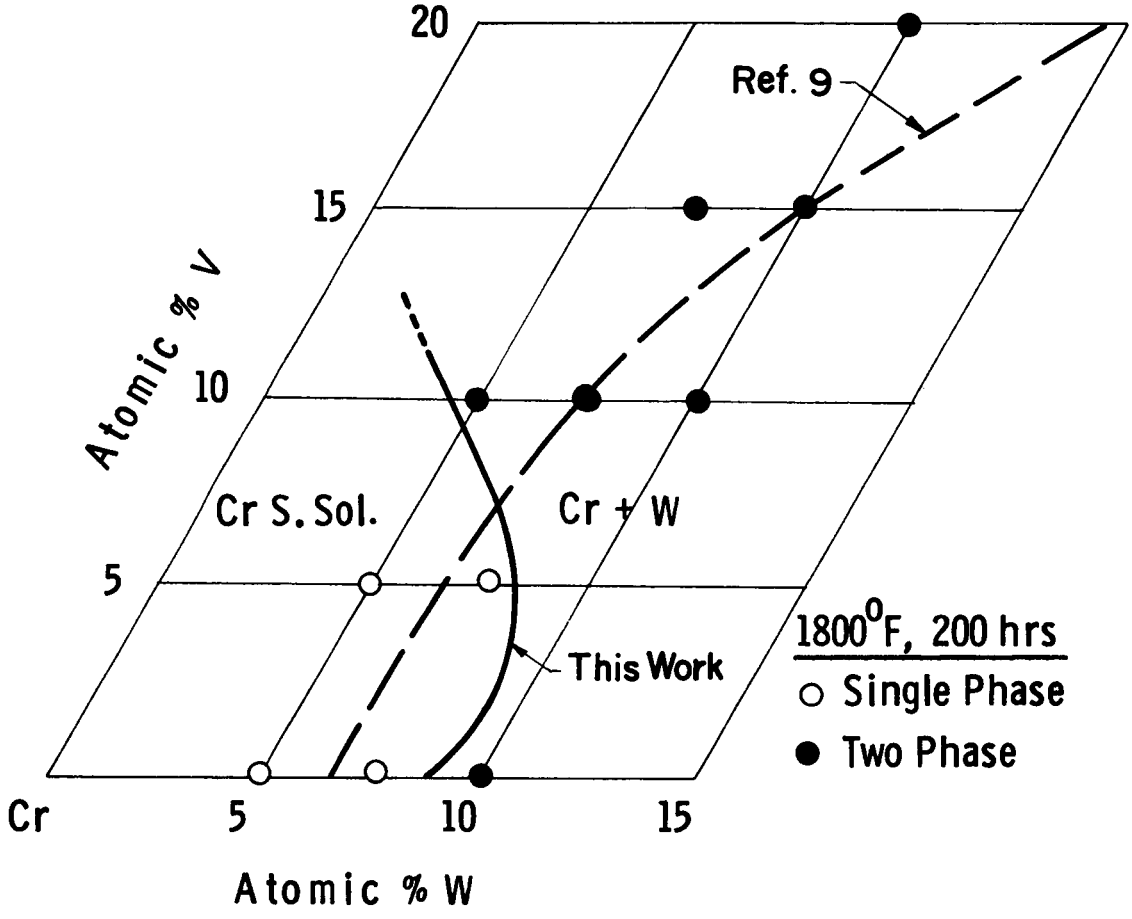

Figure 10. Cr-rich corner of the Cr-W-V equilibrium diagram at 1800°F, showing location of experimental alloys and extent of W solubility according to English [9].

A. Cr-14.2Re-10.4Co

Grain-boundary sigma

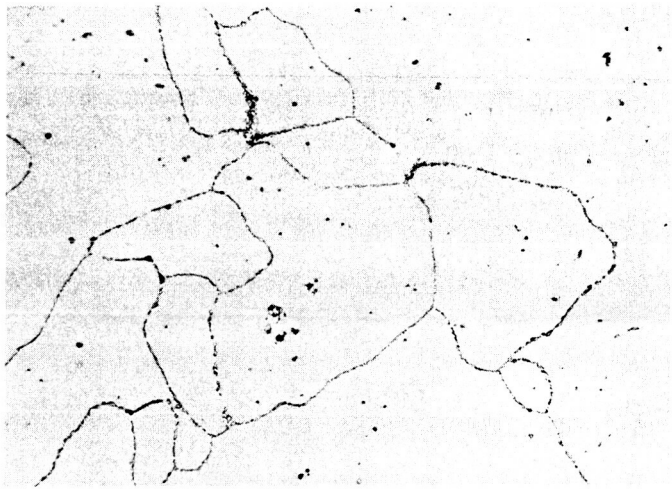

M9871 250X

B. Cr-11.0Re-17.2Co

Approximately 50% sigma

M7973 250X

C. Cr-11.0Re-23.1Co

Approximately 80% sigma

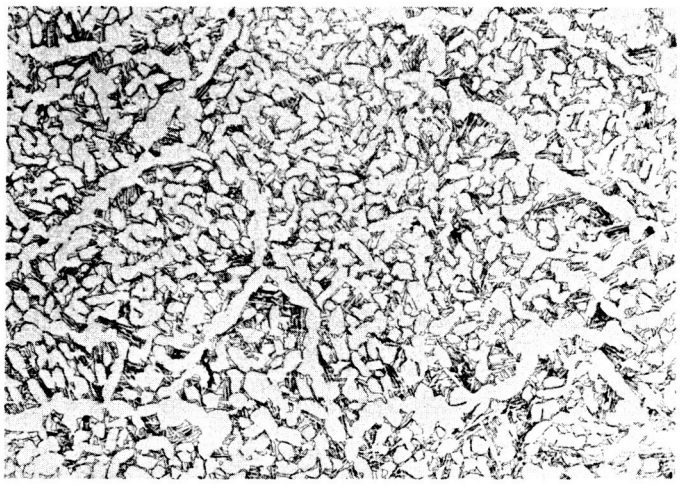

M7974 250X

Figure 11. Effect of 100-hour aging at 1650°F on the structure of Cr-Re-Co alloys at indicated atomic concentrations. Etched 10% oxalic acid.

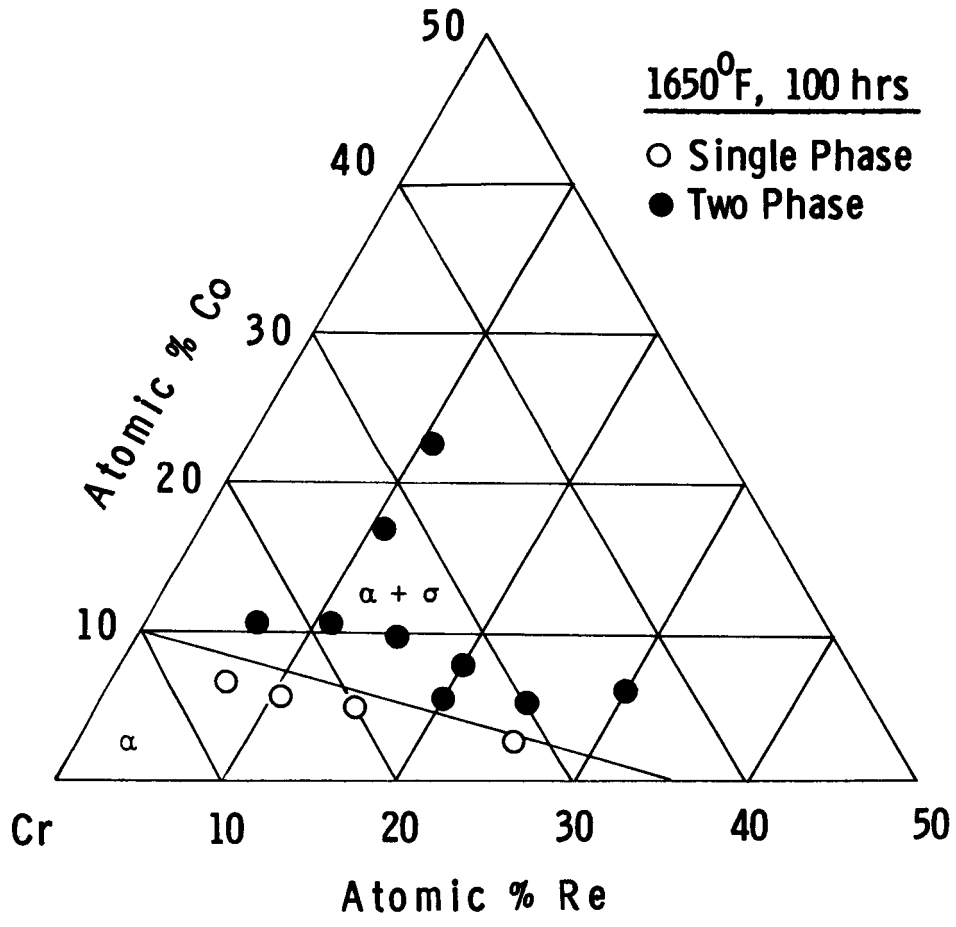

Figure 12. Cr-rich corner of the Cr-Re-Co equilibrium diagram at 1650°F, showing extent of chromium solid solutions.

TABLE 13

COMPOSITIONS OF COMPLEX Cr-Mo-MC-La ALLOYS AND METALLOGRAPHIC OBSERVATIONS AFTER OXIDATION

Alloy Compositions (Atomic %)	Oxidized 24 Hrs. @ 2400°F (As Cast)			Oxidized 100 Hrs. @ 2100°F (As Swaged)		
	Total Wt. Change mg/cm^2	Net Wt. Change mg/cm^2	Remarks	Hardness DPH, 100 Gm. Center	Edge (.001")	Remarks
0.4Zr-0.2Ti-0.4C-0.3La	2.8	-1.9	Little or no nitride	316	290	No nitride
0.6Ti-0.4C-0.3La	11.5	-24.2	Little or no nitride	340	364	Little or no nitride
0.6Zr-0.4C-0.3La	3.2	1.5	Nitride needles	340	358	Little or no nitride
0.6Cb-0.4C-0.3La	20.4	-9.75	Intergranular nitride + needles	358	364	Slight nitride (irregular)
0.6Cb-0.4C-0.4La	30.2	-54.5	Extensive nitride	333	393	Small amt. internal nitride
0.6Ta-0.4C-0.3La	34.0	-30.1	Extensive nitride	327	346	Slight intergranular nitride
0.3Ta-0.3Hf-0.4C-0.3La	19.0	-52.0	Extensive nitride	322	295	Slight intergranular nitride
0.6Hf-0.4C-0.3La	5.1	-8.1	Little or no nitride	351	340	Little or no nitride

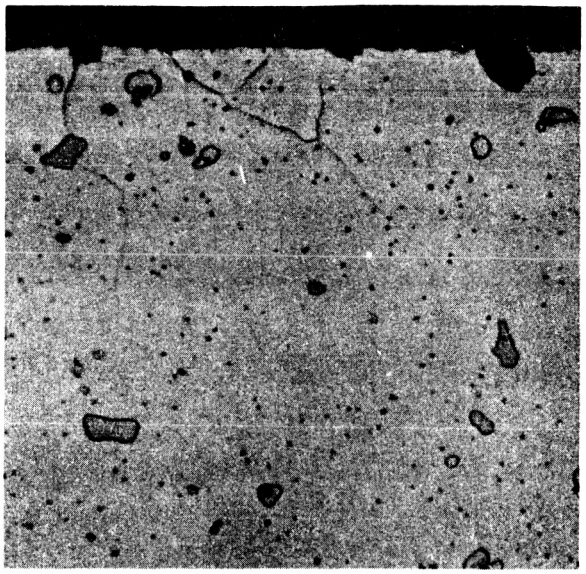

3871 1000X

A. Cr-1Zr-.4C-.1Y at 1500°F

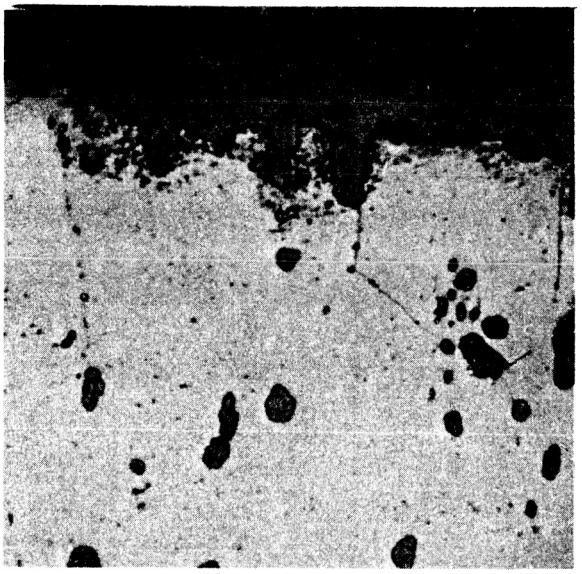

3698 1000X

B. Cr-1Zr-.4C-.1Y at 2100°F

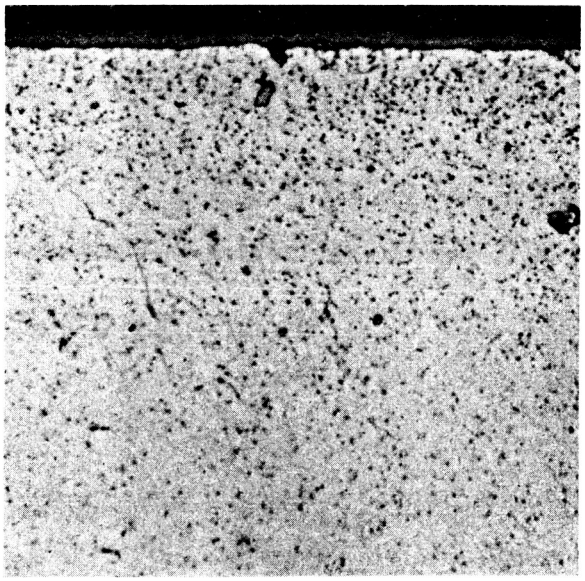

2546 1000X

C. Cr-1Cb.4C-.1Y at 1500°F

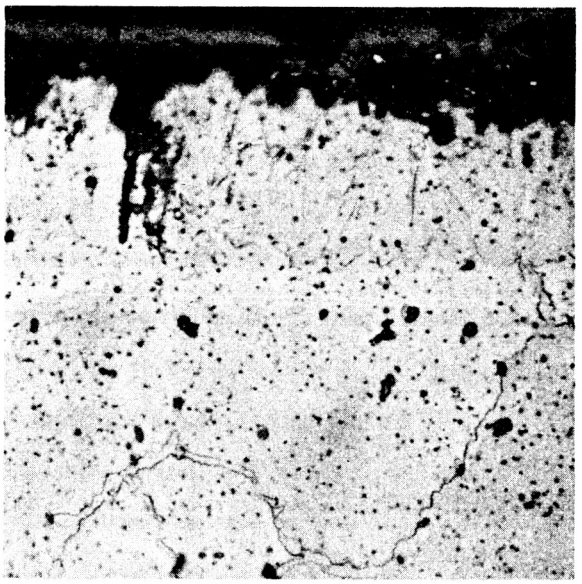

3838 1000X

D. Cr-1Cb-.4C-.1Y at 2100°F

Figure 13. Dilute Cr-Y alloys containing ZrC and CbC dispersions after 100-hour air oxidation at indicated temperatures. Nominal compositions - atomic %. Etched in Kromic acid.

A. Cr-3Cb-.1Y Aged 2200°F/5Hrs

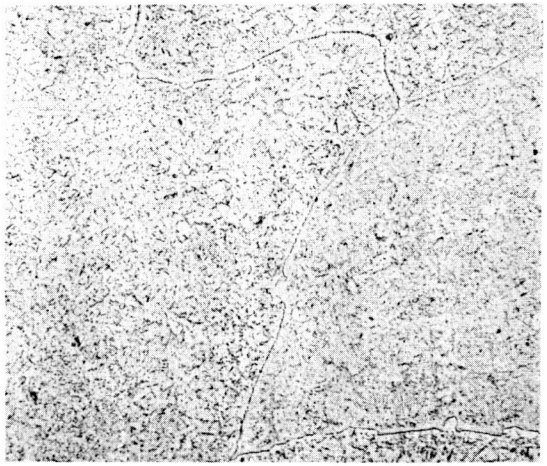

F1590 250X

C. Cr-2Si-.1Y Aged 2200°F/5Hrs

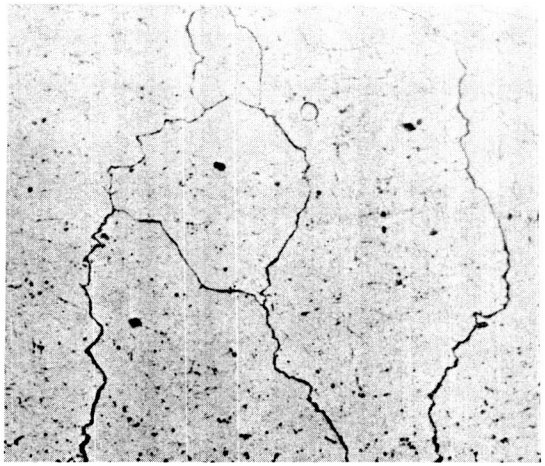

F1825 250X

E. Cr-3Cb-2Si-.1Y Aged 2200°F/5Hrs

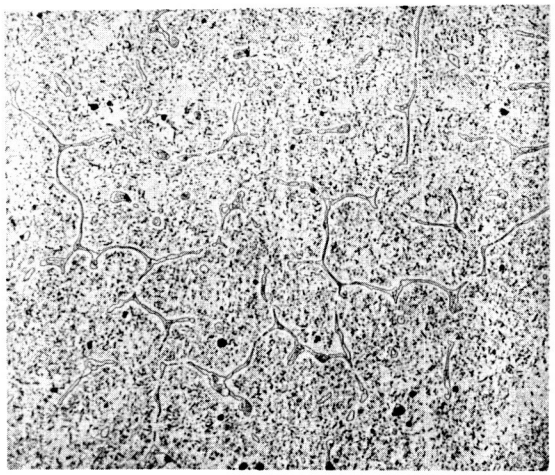

F1598 250X

B. Cr-3Cb-.1Y Oxidized 2100°F/100Hrs

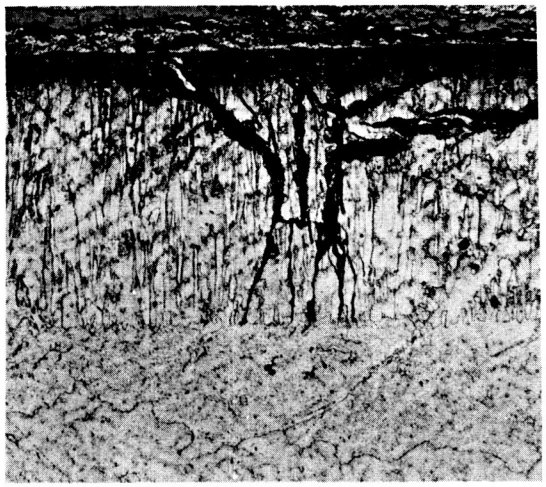

F1821 100X

D. Cr-2Si-.1Y Oxidized 2100°F/100Hrs

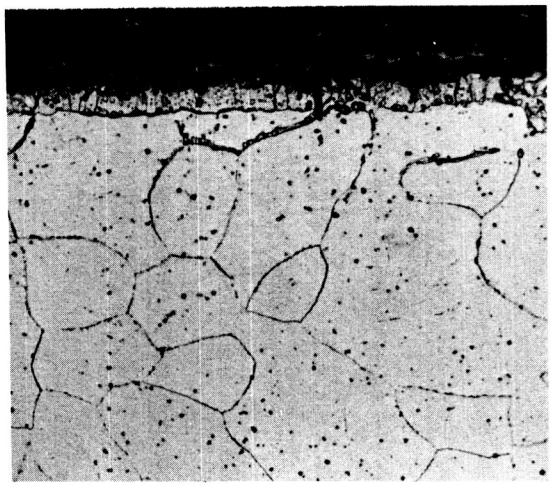

F1823 250X

F. Cr-3Cb-2Si-.1Y Oxidized 2100°F/100Hrs

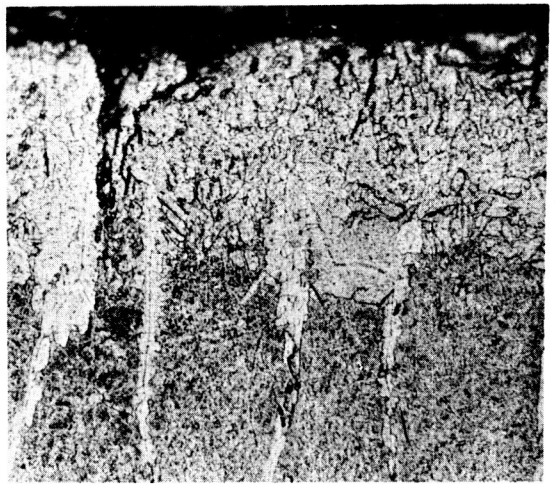

F1826 250X

Figure 14. Effects of aging and of oxidation on the structure of alloys in the Cr-Y-Cb-Si system. Etched Kromic acid.

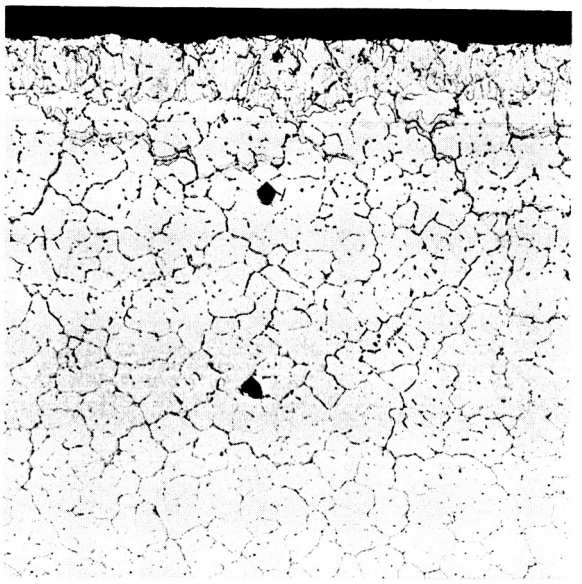

6917 100X

A. Cr-ZTC 100Hrs at 2100°F

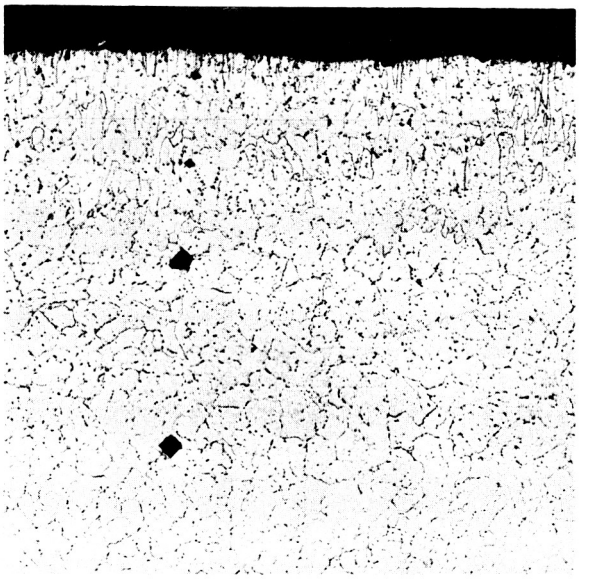

6916 100X

B. Cr-ZTC 24Hrs at 2400°F

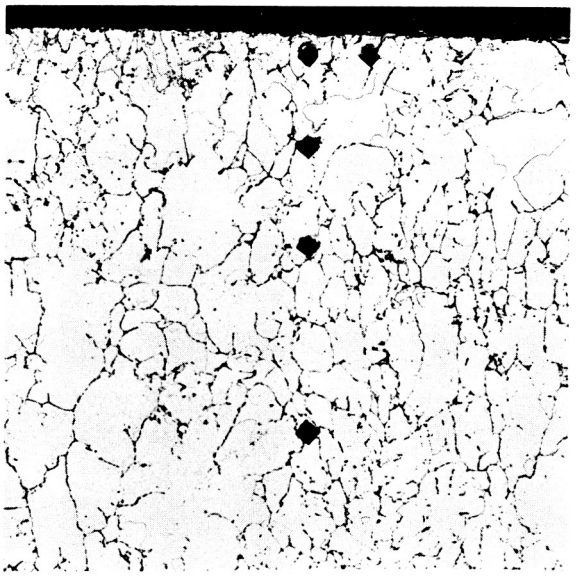

6919 100X

C. Cr-0.2La-ZTC 100Hrs at 2100°F

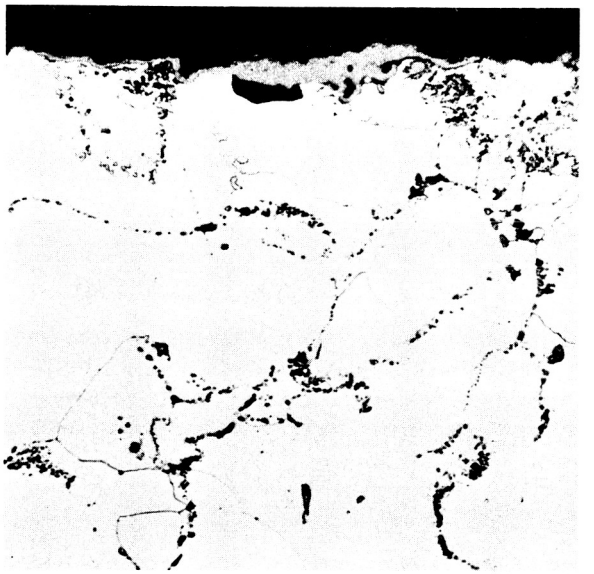

7238 500X

D. Cr-0.2La-ZTC 24Hrs at 2400°F

Figure 15. Effects of 0.2 atomic percent La on the air oxidation of Cr-ZTC alloy. Etched 10% oxalic acid.

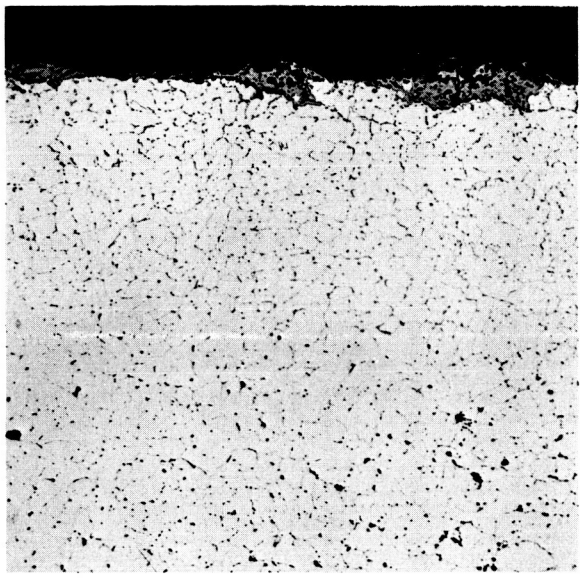

6921 100X

A. Cr-.2La-TiC 24Hrs at 2400°F

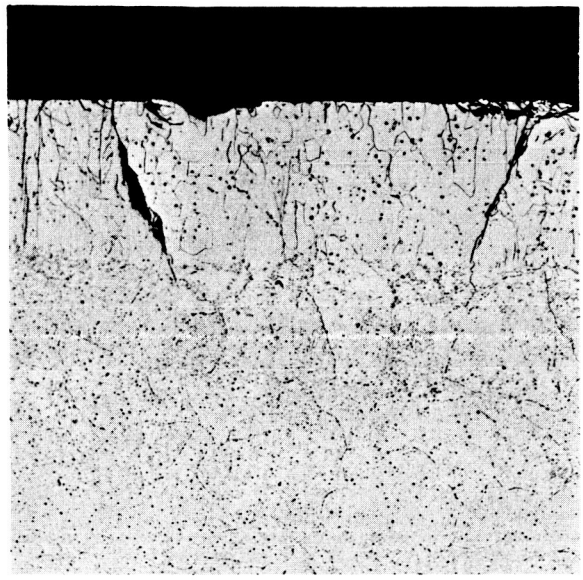

6924 100X

B. Cr-.2Pr-CbC 24Hrs at 2400°F

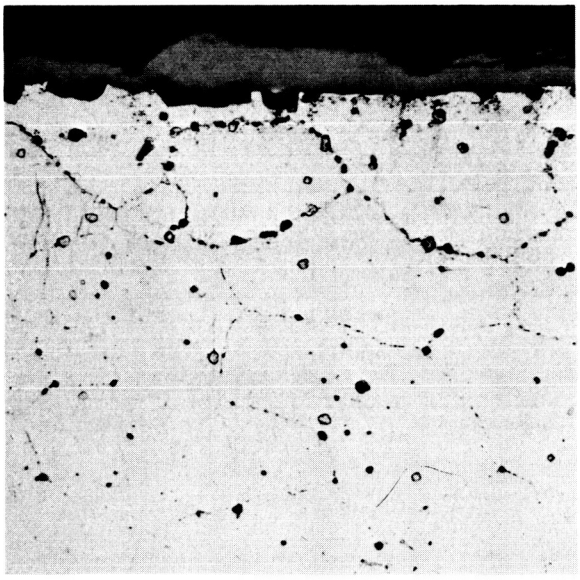

7240 500X

C. Cr-.5La-CbC 24Hrs at 2400°F

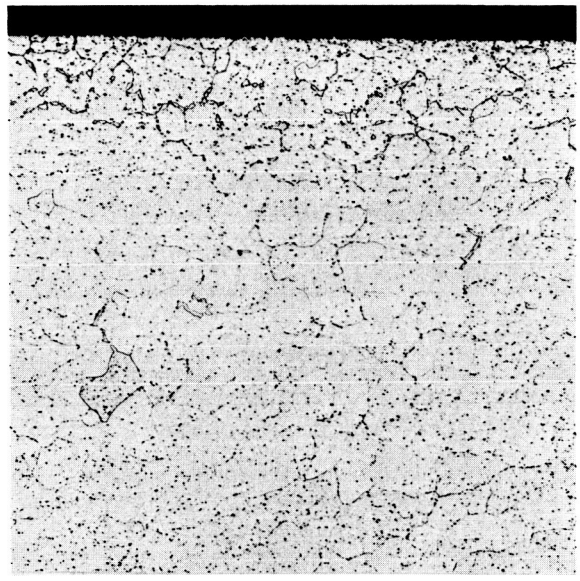

6927 100X

D. Cr-.5La-CbC 100Hrs at 2100°F

Figure 16. Effects of La and Pr additions on the air oxidation of Cr-TiC and Cr-CbC alloys. Etched 10% oxalic acid.

A. Cr-4Mo-.3La-.6Zr-.4C

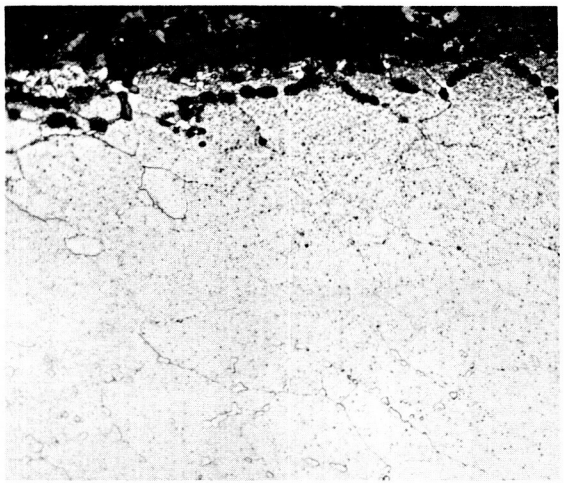

F2141 250X

C. Cr-4Mo-.3La-.4Zr-.2Ti-.4C

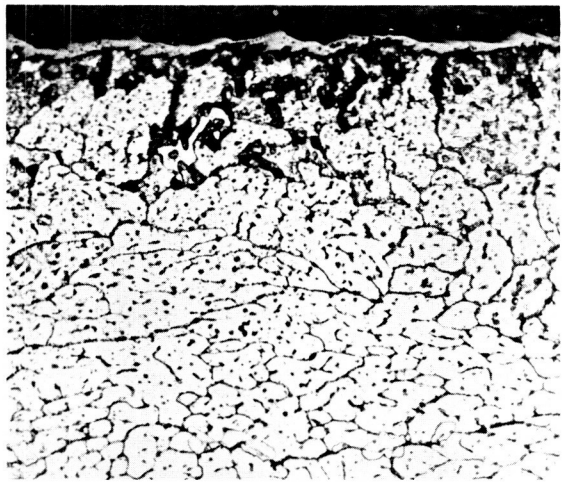

F2138 250X

E. Cr-4Mo-.3La-.6Ta-.4C

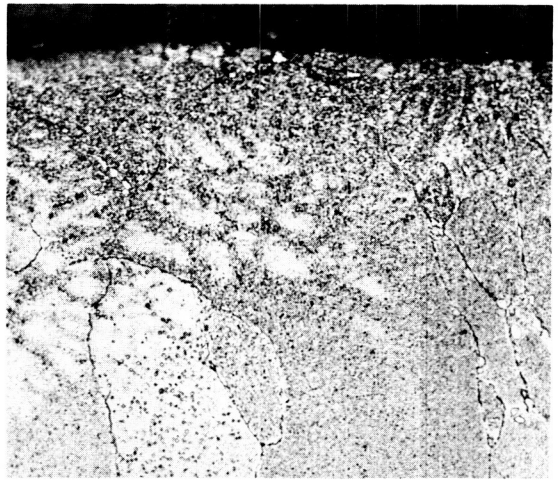

F2143 250X

B. Cr-4Mo-.3La-.6Hf-.4C

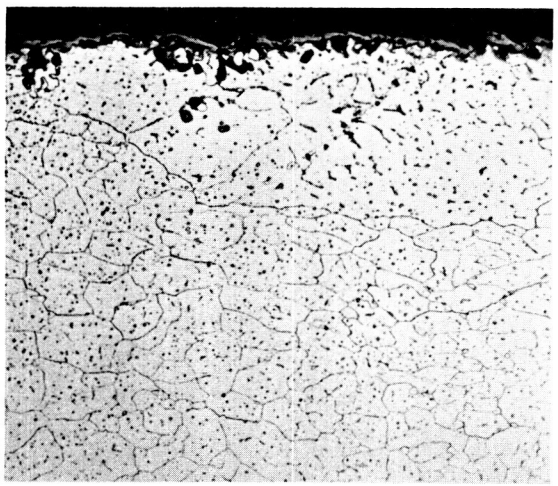

F2145 250X

D. Cr-4Mo-.4La-.6Cb-.4C

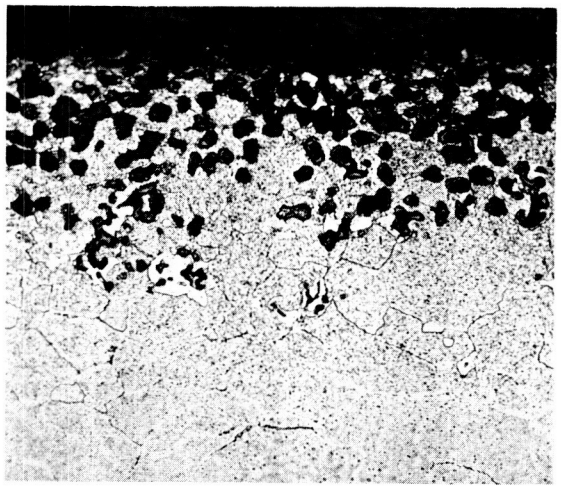

F2142 250X

F. Cr-4Mo-.3La-.3Ta-.3Hf-.4C

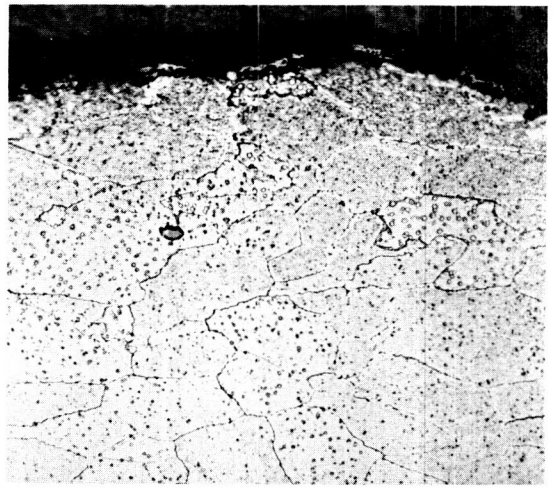

F2144 250X

Figure 17. Cr-4Mo-La alloys with various carbide dispersions after 100-hour air oxidation at 2100°F. Nominal compositions in atomic percent. Etched Kromic acid.